# AN EXPERIMENTAL STUDY OF STEAM CONDENSATION ON A SINGLE HORIZONTAL TUBE

Derry Thomas Pence

Report Number---NPS69-78-002

# NAVAL POSTGRADUATE SCHOOL
## Monterey, California


# THESIS

AN EXPERIMENTAL STUDY OF STEAM CONDENSATION

ON A SINGLE HORIZONTAL TUBE

by

Derry Thomas Pence

March 1978

Thesis Advisor: P. J. Marto



Prepared for: Naval Sea Systems Command
Washington, D.C.

# REPORT DOCUMENTATION PAGE

READ INSTRUCTIONS BEFORE COMPLETING FORM

| | |
|---|---|
| 1. REPORT NUMBER: NPS69-78-002 | 2. GOVT ACCESSION NO. |
| 3. RECIPIENT'S CATALOG NUMBER | |
| 4. TITLE (and Subtitle): An Experimental Study of Steam Condensation on a Single Horizontal Tube | 5. TYPE OF REPORT & PERIOD COVERED: Master's Thesis, Technical Report; March 1978 |
| 6. PERFORMING ORG. REPORT NUMBER | |
| 7. AUTHOR(s): Derry Thomas Pence | 8. CONTRACT OR GRANT NUMBER(s): N0002477-WR74134 |
| 9. PERFORMING ORGANIZATION NAME AND ADDRESS: Naval Postgraduate School, Monterey, CA 93940 | 10. PROGRAM ELEMENT, PROJECT, TASK AREA & WORK UNIT NUMBERS |
| 11. CONTROLLING OFFICE NAME AND ADDRESS: Naval Sea Systems Command, Washington, D. C. | 12. REPORT DATE: March 1978 |
| | 13. NUMBER OF PAGES: 102 |
| 14. MONITORING AGENCY NAME & ADDRESS(if different from Controlling Office): Naval Postgraduate School, Monterey, CA 93940 | 15. SECURITY CLASS. (of this report): Unclassified |
| | 15a. DECLASSIFICATION/DOWNGRADING SCHEDULE |

16. DISTRIBUTION STATEMENT (of this Report)

Approved for public release; distribution unlimited.

17. DISTRIBUTION STATEMENT (of the abstract entered in Block 20, if different from Report)

18. SUPPLEMENTARY NOTES

19. KEY WORDS (Continue on reverse side if necessary and identify by block number)

20. ABSTRACT (Continue on reverse side if necessary and identify by block number)

An experimental test facility capable of investigating plain and enhanced horizontal tubes was built. The test facility consists of an electric boiler, test condenser and associated piping for steam, condensate and cooling water. Performance of the test condenser was checked at a steam pressure of 3 psia with cooling water velocities ranging from 5 to 25 ft/sec.

Condensation data was obtained for a single, 0.625 inch outside diameter, 90-10 copper-nickel tube in a simulated tube bundle to determine the overall, inside and outside heat transfer coefficients. The overall heat transfer coefficient was determined directly from experimental data, and the Wilson Plot technique was used to determine the inside and outside heat transfer coefficients.

The experimentally obtained values for the inside heat transfer coefficient are within 5 percent of the theoretical values predicted by the Sieder-Tate equation. The experimental values obtained for the outside heat transfer coefficient are within 8 percent of the theoretical values predicted by the Nusselt equation.

Approved for public release; distribution unlimited.

# An Experimental Study of Steam Condensation on a Single Horizontal Tube

by

Derry Thomas Pence
Lieutenant, United States Navy
B.S., University of Arizona, 1970

Submitted in partial fulfillment of the
requirements for the degree of

MASTER OF SCIENCE IN MECHANICAL ENGINEERING

from the

NAVAL POSTGRADUATE SCHOOL
March 1978

ABSTRACT

An experimental test facility capable of investigating plain and enhanced horizontal tubes was built. The test facility consists of an electric boiler, test condenser and associated piping for steam, condensate and cooling water. Performance of the test condenser was checked at a steam pressure of 3 psia with cooling water velocities ranging from 5 to 25 ft/sec.

Condensation data was obtained for a single, 0.625 inch outside diameter, 90-10 copper-nickel tube in a simulated tube bundle to determine the overall, inside and outside heat transfer coefficients. The overall heat transfer coefficient was determined directly from experimental data, and the Wilson Plot technique was used to determine the inside and outside heat transfer coefficients.

The experimentally obtained values for the inside heat transfer coefficient are within 5 percent of the theoretical values predicted by the Sieder-Tate equation. The experimental values obtained for the outside heat transfer coefficient are within 8 percent of the theoretical values predicted by the Nusselt equation.

TABLE OF CONTENTS

LIST OF TABLES

LIST OF FIGURES

## NOMENCLATURE

$A_o$ - outside surface area of test tube ($ft^2$)

$C_i$ - coefficient of Sieder-Tate equation

$c_p$ - specific heat (BTU/lbm-$^oF$)

D - inside diameter of pipe (in)

$D_o$ - outside diameter of test tube (ft)

$D_i$ - inside diameter of test tube (ft)

$d_e$ - equivalent diameter (ft)

f - friction factor

$F_A$ - expansion-contraction factor for inside area of pipe

$F_M$ - manometer correction factor

$g_c$ - dimensional conversion factor (ft-lbm/$lb_f$-$sec^2$)

$G_{max}$ - mass velocity (lbm/hr-$ft^2$)

$h_i$ - inside heat transfer coefficient (BTU/hr-$ft^2$-$^oF$)

$h_o$ - outside heat transfer coefficient (BTU/hr-$ft^2$-$^oF$)

$h_{oN}$ - Nusselt heat transfer coefficient (BTU/hr-$ft^2$-$^oF$)

$h_c$ - condensate film heat transfer coefficient (BTU/hr-$ft^2$-$^oF$)

$\bar{h}$ - average heat transfer coefficient (BTU/hr-$ft^2$-$^oF$)

$h_N$ - manometer deflection (inches of water)

$h_{fg}$ - latent heat of vaporization (BTU/lbm)

k - thermal conductivity (BTU/hr-ft-$^oF$)

L - effective tube length (ft)

$m_c$ - cooling water mass flow rate (lbm/hr)

$m_s$ - steam mass flow rate (lbm/hr)

N - constant, equal to 2835

$\bar{Nu}$ - average Nusselt number

$Nu_N$ - Nusselt number

Pr - Prandtl number

Re - Reynolds number

$r_i$ - inside radius of test tube (ft)

$r_o$ - outside radius of test tube (ft)

$R_w$ - wall resistance (hr-ft$^2$-$^oF$/BTU)

S - constant factor for Annubar element

$T_{ci}$ - inlet cooling water temperature ($^oF$)

$T_{co}$ - outlet cooling water temperature ($^oF$)

$T_f$ - film temperature ($^oF$)

$T_s$ - steam temperature ($^oF$)

$T_w$ - test tube wall temperature ($^oF$)

$\Delta T_{LM}$ - log mean temperature difference ($^oF$)

$U_o$ - overall heat transfer coefficient (BTU/hr-ft$^2$-$^oF$)

U - steam velocity above test tube (ft/sec)

V - velocity (ft/sec)

Va - gas adiabatic compression factor

$W_n$ - mass flow rate (lbm/hr)

$\delta$ - uncertainty

$\varepsilon$ - roughness height (inches)

$\mu$ - dynamic viscosity (lbm/ft-hr)

$\gamma_f$ - specific weight ($lb_f/ft^3$)

$\rho$ - density (lbm/ft$^3$)

$\nu$ - kinematic viscosity (ft$^2$/hr)

Subscripts:

f - film

v - vapor

w - wall

ACKNOWLEDGEMENTS

The author wishes to express his appreciation to his thesis advisor, Dr. Paul J. Marto, for his guidance and understanding. I also wish to extend a special note of appreciation to Mr. Ken Mothersell, Mr. James G. Selby and Mr. Thomas Christian, for without their efforts this project would never have been completed. Also, I wish to thank Mr. George Bixler for his assistance in machining high tolerance components.

Also, the author wishes especially to thank his family for their understanding and undying support during this period.

# I. INTRODUCTION

## A. BACKGROUND INFORMATION

Due to advances in the design of both boilers and turbomachinery, the design of condensers has gained in importance. However, improvement in operating steam plant condensers has not matched that of boilers or turbomachinery. To date, increased power output has meant increased condenser size; and to prevent the condenser from becoming the controlling factor in steam power plant design, this trend must be reversed.

In marine applications, the steam power plant continues to be a very prominent system. Although alternate power systems such as diesel and gas turbine engines have reduced the use of fossil fuel fired steam power plants, nuclear power plants have expanded in use. In Naval applications, in particular, significant attention is being directed toward the weight per shaft horsepower ratio, and because steam power plants, both conventional and nuclear, are widely applied, advances in condenser design must be investigated.

H. T. Search [1] conducted an investigation into present condenser design processes and into the feasibility of enhancing heat transer in Naval condensers. He found that the design of condensers is very conservative. In general, only smooth tubes of copper-nickel are in use today, but interest in heat transfer enhancement techniques has been increasing. The feasibility of improving condenser performance exists, and there is reason to believe that changes in tube geometry will lead to attractive improvements in performance.

B. GEOMETRIC TUBE ENHANCEMENT METHODS

A great deal of research has been done in the area of heat transfer augmentation. Bergles [2,3] has compiled extensive works in single phase and two-phase heat transfer augmentation. He categorized augmentation techniques into three areas:

Passive Techniques, consisting of

Treated surfaces,

Rough surfaces,

Extended surfaces,

Enhanced tubes,

Displaced enhancement devices,

Swirl flow devices,

Coiled tubes,

Surface tension devices,

Additives for liquids (liquid, solid, gas) and

Additives for gases (liquid, solid),

Active Techniques, consisting of

Mechanical aids,

Surface vibration,

Fluid vibration,

Electric fields,

Injection, and

Suction, and

Compound Techniques, consisting of any combination of the above categories or subcategories.

Bergles [2,3] indicates that much fundamental work remains to be done in each of these areas. The passive technique of enhanced tubes

will be addressed here because this approach to heat transfer enhancement is more pertinent to this study.

J. Palen, et al [4], in January 1971, published a report for Heat Transfer Research, Inc. in which they compared the steam condensing performance characteristics of Turbotec tubing and plain tubing. The test tubes were 1 inch outside diameter with the plain tube made out of 90-10 copper-nickel and the Turbotec tube made out of 97.5 percent copper. The test condenser had a total of 196 tubes with 16 vertical rows. The steam pressure was varied between 55 and 105 psig. The cooling water velocity varied between 1.5 and 4 ft/sec. To insure filmwise condensation, all tubes were baked in a large oven at 500$^{o}$F for 1 hour to remove residue. The experimental results show that for a given Reynolds number the friction factor for a Turbotec tube is from 10 to 15 times that of a smooth tube. On the basis of total bundle performance, the heat transfer rate was increased by a factor of 2.5 using the Turbotec tubes compared to the plain tubes.

D. M. Eissenberg [5], in 1972, performed an extensive study of condenser tube heat transfer coefficients using a multi-tube bundle. The primary objective was to study the effect of condensate rain and gas concentration on the heat transfer coefficient. A secondary objective was to verify the performance of enhanced tubes on increasing the heat transfer coefficient as compared to smooth tubes. For the enhanced tube tests, 90-10 copper-nickel rope tubes were used. Saturated steam in the range of 160$^{o}$ to 230$^{o}$F was used in the test. The results of these tests with the roped tubes yielded a value of the heat transfer coefficient 1.9 times that of a smooth tube, but with a corresponding increase in pressure drop across the tubes.

In 1973, I. H. Newson and T. K. Hodgson [6], in a paper presented before the International Symposium on Fresh Water from the Sea, discussed the effect of various tube geometries on both single phase and two-phase heat transfer. The test facility allowed for the testing of a single tube in a vertical orientation, condensing steam at atmospheric pressure. The different tube types were 4 and 8 start, swaged helical (a,c); 4 start, positive indentation helical (b); 8 start, longitudinal wave (d); and 16 and 30 start, multifluted (e,f). A comparison of the results for the enhanced tubes to a smooth tube was made at a cooling water velocity of 5 ft/sec, and the results were tabulated in the table shown in Table I. The multifluted tube, types e and f, had the best average overall performance ratio of 0.9. The overall coefficient ratio for these tubes was from 1.736 to 2.036 and the pressure drop ratio was from 1.47 to 2.515. They concluded that of the total enhancement for a tube, a greater proportion is being obtained by the enhancement on the condensing side rather than on the tube side. For a horizontal installation the enhanced tubes would derive all of their enhancement from the increase in the tube side coefficient; and therefore, the 4 or 8 start, swaged helical or the 4 start, positive indentation helical should be used.

A. P. Watkinson, et al [7], in 1973, performed tests on 18 Noranda Forge-fin tubes (Figure 2) using water on the tube side and steam on the shell side. The test facility allowed for the testing of a single, horizontal tube at atmospheric pressure or slightly higher. The inlet water temperature was adjusted to maintain a positive steam pressure, and flow rates were varied from 0.5 to 30 U. S. gallons per minute. Each tube tested was cleaned with sodium dichromate pickling solution and well

rinsed with water prior to installation. High spiral fin tubes (fin height/inside diameter $\geq$ 0.065), low spiral fin tubes (fin height/inside diameter $\leq$ 0.05) and straight fin tubes were tested. In comparing the friction factors of the test tubes to those of a smooth tube in the fully turbulent region, the values for high spiral fin tubes were 2.25 times as great, the values for low spiral fin tubes were 2.0 times as great and the values for straight fin tubes were 1.75 times as great. The greatest heat transfer enhancement as compared to a smooth tube was achieved by a high spiral fin tube with an outside diameter of 1.25 inches. At a Reynolds number of 10,000, enhancement of 170 percent was achieved, and at a Reynolds number of 100,000 an enhancement of 42 percent was achieved. When comparing experimental results to smooth tube results and using as a criteria constant pumping power, the 1.25 inch outside diameter tube exhibited the best enhancement for a Reynolds number of 25,000. The high spiral fin tubes exhibited the best heat transfer enhancement, particularly tubes with an outside diameter of 1.25 inches or greater.

In 1974, J. P. Catchpole and B. C. H. Drew [8] conducted a series of tests on five tubes of varying geometry. The tubes were made by rolling radial grooves in a plain tube (Figure 3). The test tubes were constructed from 70-30 copper-nickel tubing with various groove depths. The test facility allowed for the testing of a single tube or a bundle of tubes. Steam was supplied at two psia, and the steam was not allowed to impinge directly on the test tube, thus simulating a row of tubes below the top row in a bundle. To allow for comparison of results, all tests were conducted with a cooling water velocity of 10 feet/second. Also, all heat transfer coefficients and friction factors were calculated

as if the tube being tested were a standard plain tube. All five tube geometries tested yielded approximately 40 percent improvement on the overall heat transfer coefficient when compared to a smooth tube. The percentage increase in the friction factor of the test tubes over that of a smooth tube ranged from 33 percent to 264 percent. The relative contribution to improvement in the steam-side and water-side coefficients varied considerably between geometries. The tube with the smallest groove width (1.40 mm) had roughly equivalent improvement in both steam-side and water-side coefficients. The remaining tubes had approximately the same groove width, 2.3 mm, and had larger improvements in the water-side coefficient. Tests were also conducted on tube bundles to investigate the effect of condensate inundation and non-condensable gases. The results of these tests showed that the geometrically enhanced tubes improved the overall heat transfer coefficient between 25 and 50 percent with respect to a plain tube.

In 1975 in a paper for presentation before the 15th National Heat Transfer Conference, E. H. Young, J. G. Withers and W. B. Lampert [9] compared corrugated condenser tubes produced by the Wolverine Division of Universal Oil Products (Figure 4) to a smooth tube. Two types of tubes were tested: 5/8 inch outside diameter copper tubes and 1.0 inch outside diameter 90-10 copper-nickel tubes. Both types of tubes were tested in a bundle configuration with a 1.25 spacing to diameter ratio for the 1.0 inch tubes and a 1.4 spacing to diameter ratio for the 5/8 inch tubes. Two steam temperatures, 100°F and 212°F, were used for the tests. Under isothermal conditions, the tubeside pressure drop for the corrugated tubes was five times that of the smooth tubes for both types of tubes. The inside, water-side, heat transfer coefficient for the

1.0 inch corrugated tube was 2.2 times that of the smooth tube, while the 5/8 inch corrugated tube's value was 2.7 times that of the smooth tube. There was no enhancement of the outside, steam side, heat transfer coefficient. The results of the design study indicated that the corrugated tube design would give savings in tubing weight, bundle or stage length and number of tubes per bundle; and the net effect would be significant cost savings.

In a progress report dated 31 July 1976, R. R. Rothfus [10] of Carnegie-Mellon University reported on the results of internally finned tubes of two types of materials, aluminum and copper. The test facility consisted of a single tube mounted horizontally between two calming sections with electrical heating elements attached to the outside surface of the tube. The amount of energy applied was controlled by a variac. At a cooling water velocity of 10 ft/sec, the friction factor of the fluted copper tube was 1.4 times that of the smooth tube. The enhancement of the waterside heat transfer coefficient at a water velocity of 10 ft/sec was 1.33 times that of the smooth tube. For the same water velocity, the enhancement for the fluted aluminum tube was 1.5 times that of the smooth tube. It was concluded that it would be economically feasible to use these tubes when the Colburn j factor to friction factor ratio (2j/f) exceeds 1.0. In these tests the value achieved was 1.3.

Yorkshire Imperial Metals [11] released a technical memorandum comparing two of their roped tube designs to a smooth tube. Tests were conducted with the following parameters held constant: steam temperature at $200^{o}F$; total heat transferred approximately $4.51 \times 10^{7}$ BTU/hour; tube-side pressure drop approximately 3.48 psi; and a water flow rate of $1.26 \times 10^{6}$ lbs/hour. The test heat exchanger was constructed with 30 tubes in three vertical planes which gave an effective value of ten for the

number of vertical rows. Also, condensate could be recirculated to simulate a condenser with 10, 20, 30, 40, 50 and 60 vertical rows. The two tubes tested had four and ten grooves per inch, respectively. The cooling water velocity in the smooth tube was 5.12 ft/sec while in the test tubes it was 4.18 and 3.08, respectively. The overall heat transfer coefficient for the four groove per inch tube was 1.23 times that of the value for the smooth tube. For the ten groove per inch tube, the value was 1.30 times that of the smooth tube. The enhancement for both tests was achieved in both single and two-phase condensation. The friction factor for the four groove per inch tube was 2.03 times that of the smooth tube; while for the ten groove per inch tube, it was 4.96 times that of the smooth tube.

In summation of the literature reviewed, it is evident that only the first steps have been taken in the determination of an optimum tube geometry for enhanced condenser heat transfer. It is further evident that more experimental research on marine condenser heat transfer enhancement possibilities is justified. Once an optimum design has been determined, tests will have to be conducted under various steam conditions for best application for the Navy.

## C. PURPOSE OF THE STUDY

Because of the increased interest by the U. S. Navy in the possibility of applying enhanced heat transfer technology to the design of marine condensers, it is necessary to have a basis whereby various heat transfer approaches can be compared to one another and to a common reference, utilizing identical test conditions.

Geometric enhancement of tubes, as described in the previous section, has been demonstrated to be an effective method of improved heat transfer

in condensers, but there is no valid basis for comparison between the various research that has been done. Each of these research studies concerned itself primarily with only one type of tube and utilized different test procedures. Therefore, to be able to select the best tube geometry it was necessary to design and construct a test facility [12] in which various tube geometries could be tested under the same conditions. These conditions would be representative of existing conditions presently faced by condensers in the U. S. Navy fleet. This requires a facility that is capable of operating with a vacuum of the order of 26 inches of mercury.

The long range testing will be done with several tube geometries, both single tube and multi-tube, under various operating conditions to form a legitimate basis for comparison. The purpose of this report was to establish baseline data using a 5/8 inch outside diameter, 90-10 copper-nickel tube, which is the standard condenser tube presently in service in Naval condensers. The purpose of this performance baseline is to provide a basis for comparison between alternative tube geometries and configurations.

# II. EXPERIMENTAL APPARATUS

## A. INTRODUCTION

A. C. Beck [12] designed the test facility and completed the layout of the major system components. The machinery layout followed his recommended piping and instrumentation diagrams.

As the system was being constructed, and upon initial operation, changes to the initial design had to be made. Certain conditions which did not exist when the original design was done also forced changes to the test facility. In the description of the experimental apparatus, particular attention will be paid to changes to the original design plus identification of important valving.

## B. STEAM SYSTEM

Figure 5 is a schematic of the steam system, showing the location of all of the valves. The boiler is an electrically heated Fulton Boiler which produces saturated steam at the rate of 100 pounds/hour. From the boiler, the steam flows through a 0.75 inch diameter line to a steam separator. After the separator, the steam flows through a 1.25 inch diameter line which divides into two steam flow paths. The first steam flow path is through the steam flow meter, a throttling valve (MS-3), and the desuperheater and onto the test condenser. Steam not condensed in the test condenser is collected in an exit manifold and piped to the secondary condenser. The secondary steam flow path is through a stop valve (MS-4) directly to the secondary condenser. The purpose of the secondary steam flow path is to control the mass flow rate of steam to the test condenser.

All steam lines are insulated with 1.0 inch fiberglass insulation with the exception of the line downstream of the throttle valve (MS-3) to the test condenser. This part of the steam line was not insulated for the purpose of temperature control of the steam, which will be more fully explained in a later section.

C. TEST CONDENSER

Reference 12 gives the design criteria for the test condenser. As shown in Figure 6, the steam inlet is through the top and the steam then enters an expansion section that has three baffles. Three layers of stainless steel, 150 mesh, screen were placed above the flow straightener to provide flow resistance. After passing through the flow straightener, the steam enters a converging inlet guide section which leads to the test section and tube bundle. Steam which is not condensed passes into a manifold and is piped to the secondary condenser where it is condensed. The condensate is collected at the bottom of the condenser and then flows out of two 0.5 inch openings on either side of the test condenser to a hotwell where it is collected.

To achieve a uniform velocity distribution within the test section, two items in the original design had to be changed. The first was the insertion of the screen described above. The second change had to do with the excess steam exhaust manifold. Originally, the exhaust manifold had a single 2.5 inch opening at one end of the test condenser. But to achieve a uniform velocity profile, another opening, 1.25 inches in diameter, was made at the opposite end of the manifold (see Figure 7). A valve was inserted in the line between the new opening and where it joined the piping to the secondary condenser to provide flexibility in operation. A complete discussion of the velocity profile is provided in the test results section.

Two other problems were encountered with the condenser due to poor workmanship by the contractor. These involved the flow straightener and window frames. Originally, the flow straightener was to be a stainless steel grid, but it was unsatisfactory, and a new flow straightener was constructed by close packing 0.5 inch diameter thin walled stainless steel tubing. Under pressure testing for tightness, the window frames were found to be cracked and unsatisfactory for use. New frames were therefore constructed using stainless steel plate and stainless steel angle iron.

The test section as shown in Figure 6 has nine 0.625 inch outside diameter, 18 gauge, 90-10 copper-nickel tubes with an effective length of 36 inches. The spacing to diameter (S/D) ratio used is 1.5 because this is the most prevalent ratio in use today in Naval condensers. The center tube of the tube bundle is the only tube with cooling water passing through it. The remaining eight tubes were installed to simulate the flow pattern in a tube bundle.

Viewing windows are on the front and back of the test condenser providing a view of the entire tube bundle so that the condensation process can be observed. Two types of glass are available. One type is a standard Pyrex glass plate 0.5 inch thick. It has one drawback in that condensation can occur on the window surfaces which allows fogging, so that the mode of condensation cannot be physically observed. The other type is an Owens-Corning Pyrex glass which has a transparent electrically conducting coating applied. This glass can be heated to the saturation temperature for the prevailing pressure inside of the test condenser which prevents fogging.

The test condenser is insulated with 2.0 inches of Johns-Manville Aerotube sheet insulation to prevent heat losses through the walls of the test condenser.

## D. CONDENSATE AND FEEDWATER SYSTEMS

Figure 8 shows a schematic layout of the condensate and feedwater systems.

The condensate is collected in two hotwells, one on the test condenser and one on the secondary condenser. The hotwell for the test condenser can be isolated from the hotwell for the secondary condenser by a gate valve (C-1) so that the mass of the condensate for the test condenser can be determined.

All of the condensate must be collected in the secondary condenser hotwell to be pumped out to either the feed tank or to the condensate return line when using house steam. The pump is a centrifugal pump and must be started before the discharge valve (C-2 or C-3) is opened to insure positive flow.

When operating with the feed tank on the line, the feed pump, which takes a suction off of the bottom of the feed tank, runs continuously. Feedwater flow to the boiler is controlled by a solenoid valve (FW-3) which is activated by the low level limit switch on the boiler controls. To insure that a positive flow through the feed pump exists at all times, the valve (FW-2) on the recirculation line is positioned to maintain a minimum flow.

The feedwater temperature is maintained at 140$^{o}$F to reduce fluctuation in boiler output and to provide water at the saturation temperature for the desuperheater which is described in the secondary systems section.

The condensate lines are insulated with Johns-Manville Aerotube insulation, 0.75 inch thickness. The feedwater lines are insulated with fiberglass insulation, 0.5 inch thick.

E. COOLING WATER

The original design [12] proposed a once through cooling water system utilizing the water supply in the building. However, in order to operate at higher flow rates, and in an effort to conserve water, a closed cooling water system was installed. To achieve these higher flow rates, a 7.5 horsepower, electrically driven, centrifugal pump was installed. The secondary condenser was also supplied cooling water through its own closed system. Figure 10 is a schematic of the cooling water system.

Cooling water flow to the test condenser is controlled by valve CW-4 and is measured with a rotameter.

To insure fully developed flow at the entrance of the test condenser, the piping was reduced to 0.625 inch outside diameter tubing (same size as the test tube) at a distance of 2.5 feet ahead of the test condenser. Pressure taps were installed in the permanent piping at both ends of the test tube in accordance with the ASME Power Test Order.

Supplying cooling water to the test condenser at a constant temperature is a stringent requirement, and to achieve this in a closed system there must be a means to remove the energy absorbed during the condensation process. This was accomplished by incorporating an air-cooled heat exchanger into the system. Air was supplied to the heat exchanger by an electrically driven fan. To insure optimum water flow rate through the heat exchanger, a by-pass loop on the supply line to the test condenser was installed so that flow through the heat exchanger could be maintained at approximately 50 gallons/minute. Flow through the by-pass loop is controlled by valve CW-3 and is measured by a rotameter. The cooling water lines to the test condenser were insulated with 1.0 inch thick Johns-

Manville Aerotube insulation to aid further in maintaining a constant cooling water inlet temperature.

F. SECONDARY SYSTEMS

1. Vacuum System

A mechanical vacuum pump is used to establish subatmospheric pressure within the test condenser and the secondary condenser. The vacuum pump takes a suction on the system from the condensate discharge line of the secondary condenser. Vacuum control is achieved by the use of a vacuum regulator which induces an air leak into the system. The vacuum regulator is installed in the suction line of the vacuum pump.

2. Desuperheater

The desuperheater is a 10.5 inch diameter stainless steel can, 18 inches high, which has four nozzles inserted equidistant around the periphery of the can near the top. The nozzles are a fan type and are positioned such that the spray is downward at a 45 degree angle to allow for better mixing. The diameter of the can is greater than that of the steam line to slow the steam down and allow more residence time for the steam in the desuperheater.

As shown in Figures 5 and 8, water flow to the desuperheater is taken from the discharge of the feed pump and is maintained at approximately 140$^{o}$F. Flow is measured by a rotameter and is controlled by a gate valve (DS-1). A steam trap is located on the bottom of the desuperheater to allow for drainage of condensate. This condensate is collected in a small tank. The steam trap and tank can be isolated from the system by valve (DS-2).

G. INSTRUMENTATION

1. Flow Rate

a. Cooling water flow rate to the test condenser is determined by a rotameter with a capacity of 18.6 gallons per minute. The calibration procedure for this rotameter is in Appendix A.

b. Cooling water flow rate to the by-pass loop is determined by a rotameter with a capacity of 86 gallons per minute. The calibration procedure for this rotameter is in Appendix A.

c. Steam flow rate through the Ellison Annubar is determined by a water differential manometer. This manometer is mounted so that its angle of inclination can be varied. As the flow rate is decreased, the deflection decreases so the angle of inclination can be reduced to obtain a discernible deflection. The actual mass flow rate is calculated as shown in Appendix B.

2. Pressure

a. Boiler pressure is measured by a Bourdon tube pressure gauge.

b. The secondary condenser pressure is measured by a compound gauge.

c. The test condenser pressure is measured by two independent measuring devices, an absolute pressure transducer and a mercury manometer. According to the ASME Power Test Codes for steam condensing apparatus, the pressure lines are 0.375 inch in diameter expanding to 0.5 inch going to the measuring device. Between the measuring device and the 0.5 inch

line, a condensate collection container has been installed to eliminate the effect of the water head.

(1) The absolute pressure transducer calibration procedure is given in Appendix A. The output is displayed on an automatic digital recorder.

(2) The mercury manometer has a water column on top of the mercury and this head must be taken into account to determine the actual pressure.

3. Temperature

Three types of thermocouples are used to measure various temperatures. They are iron-constantan; copper-constantan, teflon-coated; and copper-constantan with a stainless steel sheath.

The iron-constantan and teflon coated copper-constantan thermocouples are used to monitor system operation. The iron-constantan thermocouple is used to measure the boiler steam temperature and is wired to a single channel pyrometer. The teflon coated copper-constantan thermocouples are wired to a 28 channel digital pyrometer which reads directly in degrees Fahrenheit. A list of the active channels and their outputs are contained in the Operating Procedures in Appendix B.

The stainless steel sheathed copper-constantan thermocouples are all wired to the automatic digital recorder which reads directly in degrees Celsius. These thermocouples are used to measure all temperatures required in the heat transfer calculations. A list of channels and their outputs are listed in the Operating Procedures in Appendix B. Six thermocouples, equally spaced across the test condenser, are used to measure the steam vapor temperature as shown in Figure 5. In accordance with ASME Power Test Codes for Steam Condensing Apparatus, one thermocouple

is used to determine the cooling water inlet temperature and four thermocouples are used to measure the cooling water outlet temperature as shown in Figure 9. The four thermocouples for the cooling water outlet temperature are positioned so that each thermocouple measures the temperature in an equal section of the cross sectional area of the test tube. A single thermocouple is used to measure the test tube wall temperature and is located on the bottom, outside surface of the tube in a shallow groove.

# III. EXPERIMENTAL PROCEDURE

## A. PRESSURE DROP ANALYSIS FOR TEST TUBE

### 1. Isothermal Analysis

In accordance with the ASME Power Test Codes, pressure taps of 0.31 inch in diameter were made in the cooling water line leading into and out of the test tube. The distance between pressure taps is 51.125 inches, of which 48 inches is the test tube. (See Figure 10.) The remainder consists of Swagelok fittings. Upstream of the high pressure tap, there are more than 54 diameters of straight 0.625 inch diameter tubing to insure fully developed flow entering the test section. Downstream of the high pressure tap there are over two diameters before the Swagelok fitting to insure that any disturbances transmitted to the flow do not effect the pressure reading. Upstream of the low pressure tap there are over two diameters before the Swagelok fittings to insure no effect on the pressure reading. Downstream of the low pressure tap there are over ten diameters before the piping bends to insure no effect on the pressure reading.

The pressure taps are connected to a mercury manometer and the differential pressure is obtained by recording the difference in the height of the mercury legs and compensating for the difference in the water heights.

To determine the isothermal differential pressure, water was passed through the test tube with all other systems secured to insure no temperature effects. Nine data points were taken, with the cooling water velocity ranging from 5 ft/sec to 25 ft/sec.

2. Non-Isothermal Analysis

To determine the non-isothermal differential pressure, readings were taken during system operation at each data point. These data points had a cooling water velocity ranging from 5 ft/sec to 25 ft/sec.

B. SYSTEM OPERATION

Saturated steam at 5 psig was produced in the boiler and was then passed through a throttle valve to reduce pressure. Before entering the test condenser which was kept at 3 psia, the steam passed through a desuperheating chamber to reduce the steam temperature to approximately saturation conditions. This was accomplished by injecting feedwater at 140°F at a rate of 20 lbm/hour into the superheated steam to provide good mixing.

The pressure within the test condenser was controlled by the use of a vacuum regulator valve.

The feedwater heater thermostat was set at 140°F to insure hot feedwater to the boiler and to supply water to the desuperheater.

Runs were normally made at night so that the outside air temperature was such that the cooling water temperature could be maintained at approximately 75°F. Steam flow, steam temperature and cooling water inlet temperature were the parameters that were controlled, and the cooling water velocity was varied.

C. TEST TUBE PREPARATION

The intent of this study was to study the heat transfer characteristics of 90-10 copper-nickel tubing in a filmwise condensation mode. To insure filmwise condensation, a chemical cleaning procedure was used which was a modification of a procedure used in preparing copper for

electroplating [13]. The steps in the cleaning process are as follows:

1. Prepare a solution of equal parts of ethyl alcohol and a 50 percent solution of sodium hydroxide, and heat to 180°F.
2. Apply this solution to the surface of the test tube.
3. Drain and rinse the test tube with tap water.
4. Rince thoroughly with distilled water.

To remove any deposits on the inside surface of the test tube a solution of 50 percent hydrochloric acid is used. The acid solution is applied by brush and the test tube is then rinsed thoroughly with tap water. After rinsing with tap water the tube is then rinsed with distilled water.

D. DETERMINATION OF STEADY STATE

Two parameters are used to establish when the system has achieved steady state. They are the cooling water inlet temperature and the steam vapor temperature.

The magnitude of the inlet cooling water temperature is dependent on the ambient air temperature. The air-to-water heat exchanger's effectiveness is dependent on the air temperature and the mass rate of water flow through the heat exchanger. The water mass flow rate through the heat exchanger is controlled by water flow through the by-pass loop. Therefore, once the system is put into operation, the cooling water inlet temperature will stabilize at a temperature approximately 12°F above the ambient air temperature. When this temperature is achieved and does not increase more than 1°F/hour, the inlet cooling water temperature has achieved a steady state condition.

The temperature of the steam upon exit from the boiler is approximately 230°F, and the only means of reducing the temperature to the saturation temperature corresponding to the test condenser pressure is by the desuperheater. To determine the quality of mixing of steam and water within the desuperheater, steam was passed through the test condenser without cooling water; and the temperature variation across the test condenser was found to be 2°F. With the introduction of cooling water, the steam temperature variation increased to 5°F. This temperature variation apparently occurs because of the temperature difference in the inlet and outlet cooling water temperatures. When the system is put into operation, the steam temperature variation across the test section is approximately 10°F and eventually stabilizes between 5° and 6°F. When the steam temperature variation is stabilized and the steam temperature at each location does not rise more than 0.5°F/min, steady state is achieved for the steam.

To achieve the above steady state conditions requires 1.5 to 2.0 hours of system operation. Additionally, when the cooling water mass flow rate is varied, ten to 15 minutes is required to allow the cooling water outlet temperature to stabilize.

## E. DATA COLLECTION

A data run consists of nine data points over the range of cooling water velocities from 5 ft/sec to 25 ft/sec. Data at each point is taken over a period of five minutes. Before any data is taken at any operating point, or during data taking, the test section is viewed to insure that there is no flooding of the test tube from above, either by carryover from the desuperheater or from condensation on other surfaces.

All steam temperatures and inlet and outlet cooling water temperatures are recorded in one minute intervals for each data point on the automatic digital recorder.

The steam mass flow rate is determined from measuring the differential across the steam flow measuring device on an inclined water manometer. To determine accurately the amount of steam entering the test condenser, the steam flow rate must be added to the water flow rate injected into the desuperheater. From this quantity should be subtracted the amount of condensate collected by the steam trap off the bottom of the desuperheater to define accurately the actual mass flow rate.

The cooling water mass flow rate is measured by a rotameter. Additionally the differential pressure drop across the test tube is recorded from a mercury manometer.

The pressure inside of the test section is monitored by a mercury manometer and an absolute pressure transducer whose output is recorded on the automatic digital recorder.

## F. AXIAL VELOCITY DISTRIBUTION IN TEST CONDENSER

To insure uniform condensing conditions along the total length of the test tube, it is necessary that the axial velocity distribution within the test section be uniform, or nearly so. Two methods were employed to determine the velocity distribution within the test section: flow visualization and the hot wire anemometer method.

The first step in determining the velocity distribution for a given configuration was to employ flow visualization. To obtain flow visualization, the tube sheets of the test condenser were replaced with plexiglas ends so that the interior of the test section could be illuminated. A 0.25 inch diameter copper tube with 0.0625 inch holes drilled every

two inches was passed through the test section at the same height as the top tube in the bundle (see Figure 6). A fine mist of liquid aerosol of di (2-ethylhexyl) phthalate was injected into the test section through the holes in the copper tubing. To simulate the steam flow, air was injected into the test condenser through the top opening (see Figure 6) at low velocities so as not to wash out completely the fine mist of aerosol droplets.

The second step in determining the velocity profile was to determine the magnitude of the velocity at various points along the length of the test section and at the same time across the width of the test section. This was accomplished by the use of a hot wire anemometer together with air flow to the test section. The hot wire anemometer probes were calibrated against a known pressure given in inches of water using the hot wire anemometer calibration unit. Calibration charts were generated for the probes, and they were plotted with the anemometer voltage squared versus the square root of the velocity. Because the probes were only 18 inches long, data was taken by inserting each probe in from one side, at approximately the level of the test tube (see Figure 6). Readings were taken at two inch intervals; then the probe was inserted into the opposite end, and the procedure was repeated. At four axial stations data was also recorded to determine variations in velocity across the width of the test section. To insure uniform conditions for each data point, the inlet air was maintained at 140 psig.

# IV. EXPERIMENTAL RESULTS

## A. AXIAL VELOCITY DISTRIBUTION

### 1. Flow Visualization Method

Flow visualization with the original configuration for the test condenser showed that the streamlines were directed toward the single opening in the steam exit manifold and a large stagnation region formed on the end opposite from the opening. (See Figure 7.)

In an attempt to make the streamlines more vertical, a 1.5 inch opening was made in the exit manifold as shown with dotted lines on Figure 7. This opening is joined to the steam line leading to the secondary condenser and has a valve (MS-6) installed to offer versatility in the system. Figure 11 shows an improvement in the streamlines with this modification. Stagnant regions remained, however, at both ends of the test section; therefore another change was made.

To force the flow to disperse across the entire cross section of the test condenser, three layers of stainless steel, 150 mesh wire screen was inserted above the flow straightener (see Figure 6). Figure 12 shows smaller stagnant regions and nearly vertical streamlines. Figure 13 shows a comparison of the flow with the valve, MS-6, open and closed.

### 2. Hot Wire Anemometer Method

The velocity profile for the original configuration as determined by the hot wire anemometer is shown in Figure 14. The velocity varied from a low of 7 ft/sec to over 36 ft/sec with the maximum occurring in the center of the test section. The velocity profile was not symmetric

about the centerline, but rather the air velocity decreased more rapidly on the side where there was no exit.

The velocity profile shown in Figure 15 is for the case with the two exits. It shows no real improvement in achieving uniform velocity distribution but the flow is more symmetrical about the centerline. The maximum air velocity was 32.5 ft/sec, and the minimum was 3.5 ft/sec.

The velocity profile shown in Figure 16 is for the two exit configuration with the addition of three layers of wire mesh. With both exits fully open, the velocity profile is relatively uniform throughout the test condenser. The velocity did not vary significantly across the width of the test condenser at any point checked. Therefore, the active condensation length is the total length of the test condenser.

## B. EXPERIMENTAL TUBE DESCRIPTION

Five condensation test runs were made. Prior to making these runs, several runs were made with an identical tube to determine that the system performed as desired. Table II is a list of the five test runs with a description of tube preparation and the visually observed condensation mode.

The procedures used to prepare the inside and outside surfaces of the test tube were those described in the Experimental Procedure.

## C. PRESSURE DROP ANALYSIS

### 1. Data Reduction

The test tube was compared against the performance of a smooth tube by plotting the Fanning friction factor versus Reynold's Number. The smooth tube curve was obtained from the Blasius equation, ($10^4 \leq Re \leq 10^5$) [14]:

$$f_f = (0.079/Re^{0.25}) \qquad (1)$$

The Fanning friction factor for the experimental data was obtained from the following expression:

$$f_f = \Delta p \; g_c / 2\rho V^2 \; (\frac{L}{D}) \qquad (2)$$

The experimental data indicated that the test tube did not behave exactly as a smooth tube. Therefore, the Colebrook equation [15] was used to determine the roughness height to diameter ($\varepsilon/D$) ratio for the test tube:

$$\frac{1}{\sqrt{f}} = -2 \log \left(\frac{2.51}{Re\sqrt{f}} + \frac{\varepsilon}{2.76\ D}\right) \qquad (3)$$

2. Tube Performance

As shown in Figure 17, the isothermal friction factors as calculated from equation (2) for runs 1 and 2 are slightly higher than the corresponding values calculated from the Blasius equation, equation (1). Because the test tube did not behave as a smooth tube, the experimental friction factor values were used in equation (3) to determine the $\varepsilon/D$ ratio. The $\varepsilon/D$ ratio was determined to be 0.00012, and this value is in agreement with results obtained by Bergles [2].

There was no reason to suspect any degradation in tube performance for runs 3 and 4, but during these runs the non-isothermal pressure drop increased, particularly at higher flow velocities (see Figure 17). Therefore, upon completion of run 4 a set of data was taken for the isothermal case; and, as shown in Table III, the friction factor changed slightly, starting with flow velocities of 11.5 ft/sec.

Before run 5 was made, the inside of the test tube was cleaned with a solution of 50 percent hydrochloric acid. The isothermal pressure drop test was conducted, and it was found to be in agreement with runs

1 and 2. The exact nature of the fouling was not determined nor was the cause of the fouling determined. A plausible explanation may be as follows. The tube was placed in the test condenser just prior to runs 1 and 2. After the completion of run 2, the system was shut down, and water was allowed to stand in the test tube. Runs 3 and 4 were conducted approximately five days later, and this is when the fouling was noticed. As previously mentioned, the inside of the test tube was cleaned before run 5.

The results of the non-isothermal friction factor test are very close to those of the isothermal case, as can be seen from a comparison of Figures 17 and 18. In agreement with this result, R. R. Rothfus [10] demonstrated that the friction factor in smooth tubes did not vary significantly between isothermal and non-isothermal cases.

## D. CONDENSER HEAT TRANSFER PERFORMANCE

### 1. Test Conditions

The average steam vapor temperature in the test condenser was maintained between 144.0°F and 145.9°F for all runs. Pressure in the test condenser was maintained between 3.0 psia and 3.1 psia for all runs, which means the saturation temperature in the test section was 141.5°F. This means that the steam entering the test condenser was slightly superheated, between 2.5°F and 3.5°F on the average. This level of superheat had to be tolerated because any further attempt to reduce the temperature to the saturation level led to an unacceptable amount of condensate carryover from the desuperheater. This caused a rain effect on the test tube which was felt to be detrimental to the intent of this study.

As noted earlier, an air-to-water heat exchanger was installed in the cooling water system to control the cooling water inlet temperature, but the heat exchanger was dependent on the ambient air temperature over which there was no control. The selection of the timing of the test runs was such that the ambient air temperature would not be increasing and would, at the start of each run, be approximately the same for each run. The cooling water temperature was then able to be maintained at 75°F with a variation of approximately ± 2°F for all test runs.

2. Overall Heat Transfer Coefficient

To obtain the overall heat transfer coefficient, $U_o$, the following expression was used to determine the heat transfer rate:

$$Q = m_c c_p (T_{co} - T_{ci}) \tag{4}$$

The heat transfer rate also can be determined from the following expression:

$$Q = U_o A_o \Delta T_{LM} \tag{5}$$

where

$$\Delta T_{LM} = \frac{T_{co} - T_{ci}}{\ln \frac{T_s - T_{ci}}{T_s - T_{co}}} \tag{6}$$

By equating equations (4) and (5), the following expression yields the overall heat transfer coefficient (see Figure 19):

$$U_o = \frac{m_c c_p}{A_o} \ln \frac{T_s - T_{ci}}{T_s - T_{co}} \tag{7}$$

The values for the overall heat transfer coefficient and the uncertainty band of each value are listed in Table IV. Figure 20 shows

the relationship between the overall heat transfer coefficient and the cooling water velocity. As can be seen, runs 1 and 2, which were mixed dropwise and filmwise condensation, have a consistently greater overall heat transfer coefficient than any of the other runs. Runs 3 and 4 had the lowest values of the overall heat transfer coefficient over the entire cooling water velocity range. This can be attributed to pure filmwise condensation plus the fouling discovered through the increased pressure drop. The overall heat transfer coefficients for run 5 fell between the other two curves as was expected. The values were lower than those for runs 1 and 2 due to pure filmwise consensation and were higher than runs 3 and 4 because the effect of fouling had been reduced.

Even though every attempt was made to insure that the inlet cooling water temperature remained constant, there were fluctuations as noted earlier. These fluctuations in the inlet cooling water temperature affected the overall heat transfer coefficient when the cooling water velocity in the test tube was above 19.5 ft/sec. A one degree change in the cooling water inlet temperature led to a 10 percent change in the overall heat transfer coefficient above that velocity. When the cooling water velocity was below 19.5 ft/sec, the variation in the overall heat transfer coefficient was less than 5 percent for similar changes in the cooling water inlet temperature.

The uncertainty in the overall heat transfer coefficient was dependent primarily on two quantities: the uncertainty in the cooling water mass flow rate and the uncertainty in the natural log term containing temperature differences. At low cooling water velocities, below 14 ft/sec, the dominant factor was the uncertainty in the cooling water mass flow rate, which was one percent of the mass flow rate. For flows above

this velocity, the uncertainty in temperature became the dominant factor due to the natural log term becoming increasingly smaller. A breakdown of the uncertainty analysis for the overall heat transfer coefficient is given in Appendix C.

R. M. Jackson, Jr., [16] studied the effects of cooling water velocity on the overall heat transfer coefficient for various tube materials. His results for 0.625 inch outside diameter, 90-10 copper-nickel tubes are plotted on Figure 20 and appear to correspond to the values obtained in runs 1 and 2 of this study. The tubes tested by Jackson were degreased using trichlorethylene, but no mention was made of the exact mode of condensation observed, which could explain the differences in the results of the two studies. Another factor which could contribute to the difference in results is that the steam velocity in Jackson's study was 120 ft/sec, while in this study the steam velocity was 22 ft/sec. The effect of steam velocity on heat transfer is discussed later.

3. Inside Heat Transfer Coefficient

To calculate the inside heat transfer coefficient $h_i$ for the test tube, the Sieder-Tate equation [17] was used (see Figures 21 and 22):

$$\frac{h_i D_i}{k} = C_i (Re)^{0.8} (Pr)^{0.33} (\mu/\mu_w)^{0.14} \qquad (8)$$

The value of $C_i$ was determined using the Wilson Plot technique [5].

Three curves were plotted on the Wilson Plot, Figure 23. The lower curve was determined from the data of runs 1 and 2. The upper curve was determined from the data of runs 3 and 4. The middle curve is for run 5. The slope of all three curves was determined from a least squares regression, best curve fit. The following expression equates $C_i$ to the slope of the Wilson Plot curve:

$$\text{slope} = \frac{D_o}{k\, C_i} \qquad (9)$$

For runs 1 through 4 a value of 0.0276 $\pm$ 0.0019 was obtained for $C_i$. For run 5 the value for $C_i$ was calculated to 0.0282 $\pm$ 0.0019. These values of $C_i$ were put into equation (8) to determine the inside heat transfer coefficient of the test tube. The experimental values of the inside heat transfer coefficient were independent of the mode of condensation and of the fouling. The values ranged from 1500 BTU/hr-ft$^2$-$^o$F at a cooling water velocity of 5.6 ft/sec to 4900 BTU/hr-ft$^2$-$^o$F at a cooling water velocity of 25.1 ft/sec. A complete tabulation of the inside heat transfer coefficients and uncertainties is given in Table IV.

The uncertainty in the coefficient $C_i$ is dependent on the slope of the Wilson Plot curve which is a function of the overall heat transfer coefficient, Reynolds number, Prandtl number and the dynamic viscosity of the cooling water. The uncertainty of $C_i$ was determined to be $\pm$ 6.9 percent for all three curves.

The uncertainty in the inside heat transfer coefficient is dependent primarily on two factors. The first is the uncertainty in $C_i$, which is given in the preceding paragraph. The second factor is the uncertainty in the Reynolds number which is dependent on the uncertainty in the cooling water mass flow rate, which decreases as the mass flow rate increases.

The theoretical value of $C_i$ used in the Sieder-Tate equation is 0.027, and there is good correlation between this value and the experimental values obtained in this study. In the Heat Transfer Research, Inc., report [4], a value of 0.028 was obtained for $C_i$ for smooth tubes. Withers and Young [18] tested 0.625 inch bare copper and 1.0 inch bare

90-10 copper-nickel tubes and obtained values of 0.025 and 0.026 for $C_i$ respectively. D. M. Eissenberg [19] obtained a value of 0.027 for $C_i$ in testing a smooth, 1.0 inch outside diameter aluminum tube. Correlation between these previous experimental studies and this study is therefore considered good.

4. Outside Heat Transfer Coefficient

The overall heat transfer coefficient for a single tube is considered to be composed of a series of film resistances:

$$\frac{1}{U_o} = \frac{D_o}{D_i h_i} + R_w + \frac{1}{h_o} \qquad (10)$$

Equation (10) in its more complete form contains expressions for fouling resistance and resistance due to non-condensable gases. In this study, the fouling resistance was not included because it is difficult to accurately determine the magnitude of this resistance, and it was felt that it could be controlled by cleaning the inside surface of the test tube as witnessed by the difference in the results of runs 3 and 4 versus run 5. Because of the complexity of arriving at a value for the resistance due to non-condensable gases, this resistance was also neglected. Therefore, the following expression was used to determine the experimental value for the outside heat transfer coefficient, $h_o$ (see Figure 23):

$$h_o = \frac{1}{\frac{1}{U_o} - R_w - \frac{D_o}{D_i h_i}} \qquad (11)$$

where

$$R_w = \frac{D_o \ln r_o/r_i}{2k} \qquad (12)$$

To determine the wall resistance, $R_w$, a value of 25.8 BTU/hr-ft-$^oF$ was used for the value of the thermal conductivity of the test tube. The values of the outside heat transfer coefficient and the uncertainties for each data point are tabulated in Table IV.

The uncertainty in the experimental values for the outside heat transfer coefficient is dependent on the uncertainties of the overall heat transfer coefficient, the inside heat transfer coefficient and the wall resistance. The uncertainties of the overall heat transfer coefficient have been discussed along with the uncertainties for the inside heat transfer coefficient. The uncertainty in the wall resistance was determined to be 5 percent of the wall resistance. A breakdown of the uncertainty analysis for the outside heat transfer coefficient is contained in Appendix C. Figure 24 shows how the uncertainties for the overall, inside and outside heat transfer coefficients vary with the cooling water velocity for run 5. The range of the uncertainties for the outside heat transfer coefficient was from $\pm$ 13 percent to $\pm$ 24 percent, with the highest uncertainties occurring at low cooling water velocities. In the work by Heat Transfer Research, Inc. [4], they had an uncertainty in the outside heat transfer coefficient of $\pm$ 15 percent and decided to define a corrected overall heat transfer coefficient instead of calculating inside and outside heat transfer coefficients. The corrected overall heat transfer coefficient was the experimental overall heat transfer coefficient minus the wall resistance. This approach was selected because they felt it reduced the uncertainty in the results.

The following is Nusselt's theoretical expression for the outside heat transfer coefficient [17]:

$$h_{o_N} = 0.725 \left[\frac{\rho_f(\rho_f-\rho_v)g\, h_{fg}\, k_f^3}{\mu_f D_o (T_s-T_w)}\right]^{0.25} \qquad (13)$$

In comparing the experimental values of the outside heat transfer coefficient to those predicted by Nusselt's equation, it became clear that: (1) the experimental values for runs 1 and 2 were consistently greater by more than 10 percent due to the fact that there was both filmwise and dropwise condensation occurring; (2) the experimental values for runs 3 and 4 were consistently below the theoretical value because of the increased fouling resistance (estimated to be on the order of $1 \times 10^{-4}$ hr-ft$^2$-$^{o}$F/BTU) that was not considered; (3) the experimental values for run 5 were in good agreement with the theoretical values. Figure 25 shows the relationship of the outside heat transfer coefficient for run 5 compared to the values predicted by Nusselt's equation.

Nusselt's equation, equation (13), was derived for stagnant vapor flow, and experimental values of the heat transfer coefficient can be as much as 10 percent greater than that predicted by the Nusselt expression. This occurs because as the steam moves by the condensing surface, it causes ripples, and the condensate formed can be sheared away much quicker. Several studies have been conducted to study the effect of steam velocity on the convective heat transfer coefficient.

A study by Berman and Tumanov [20] gave the effect of a downward flow of steam past a tube within a dummy bundle. The bundle had a $S/D_o$ ratio of 1.475 and the study covered steam temperatures from 75$^{o}$F to 175$^{o}$F, with mass velocities varying from 60 to 1000 lb/hr-ft$^2$. They found an increase in the condensate film heat transfer coefficient with increased steam velocity, correlating the results by the following empirical equation:

$$\frac{h_c}{h_{o_N}} = 1.0 + 9.5 \times 10^{-3} \, Re_s^{11.8/\sqrt{Nu_N}} \qquad (14)$$

where $Re_s$ is the vapor Reynolds number defined using the tube outside diameter and the superficial steam velocity, and $Nu_N$ is a condensation Nusselt number defined as:

$$Nu_N = \frac{h_{o_N} D_o}{k_f} \tag{15}$$

where $h_{o_N}$ is defined in equation (13). In this study, only one steam velocity, 22.4 ft/sec, was used and a maximum mass velocity of 671.4 lb/hr-ft$^2$ was calculated for this flow velocity. In Knudsen and Katz [14] the Reynolds number for flow across a tube bank is as follows:

$$Re = \frac{G_{max} d_e}{\mu_f} \tag{16}$$

where $d_e$ is the equivalent diameter and this was determined to be the outside diameter of the test tube. Applying equation (16) to equation (14), a value of 2641 BTU/hr-ft$^2$-$^o$F was calculated for the outside heat transfer coefficient. Figure 25 shows the relationship between this value and that obtained by the Nusselt equation.

Another study conducted by Shekriladze and Zhorzholiani [21] also observed the effect of steam flow across a horizontal tube, but their work attempted to include the effect of the afterbody of the cylinder, which up to this time had been neglected. Their results supported the hypothesis that the condensate film heat transfer coefficient increases with increasing steam velocity, correlating the results by the empirical equation:

$$\overline{Nu} = \frac{\bar{h} D_o}{k_f} = 0.64 \sqrt{Re} \left[1 + (1+1.69K)^{\frac{1}{2}}\right]^{\frac{1}{2}} \tag{17}$$

where

$$Re = \frac{U_\infty D_o}{\nu} \quad , \text{ and} \tag{18}$$

$$K = g D_o h_{fg} \mu_f / k_f (T_s - T_w) U_\infty^2 \tag{19}$$

A value of 2790 BTU/hr-ft$^2$-$^o$F was obtained for the outside heat transfer coefficient by using equation (17). One problem with using this formulation is in defining $U_\infty$ when the flow is through a tube bank. It was determined that, in this study, a representative value for the flow area above the tube would be three times that of the area between tubes; and, therefore, a value of $U_{max}/3$ was chosen for $U_\infty$ (see Figure 7).

Because equations (13), (14), and (17) are all based on pure filmwise condensation, the correlation between experimental and theoretical values for the outside heat transfer coefficient will be discussed for run 5 only. Figure 25 shows that there is good correlation between the experimental values and the values predicted by Nusselt, as noted earlier. There is no real basis in this study to indicate that the steam velocity had any real effect on the outside heat transfer coefficient.

# V. CONCLUSIONS AND RECOMMENDATIONS

## A. CONCLUSIONS

There are several conclusions to be drawn from the experimental results. The test tube did not behave as a smooth tube but rather had a roughness height to diameter ratio of 0.00012 in agreement with earlier work [2].

The overall heat transfer coefficient is less sensitive to minor cooling water inlet temperature variations when the cooling water velocity is below 19.5 ft/sec. When the cooling water velocity is greater than 19.5 ft/sec, a one degree Fahrenheit change in the cooling water inlet temperature caused a 10 percent change in the overall heat transfer coefficient, while the effect was only 5 percent for cooling water velocities below 19.5 ft/sec.

The results for run 5 are the most important because it is the only run where there was pure filmwise condensation with a minimum of fouling. The results obtained for run 5 for the inside and outside heat transfer coefficients are in good agreement with theoretical values. The values obtained for the inside heat transfer coefficient are within 5 percent of those values predicted by the Sieder-Tate equation. The values of the outside heat transfer coefficient obtained are within 8 percent of those values predicted by the Nusselt equation. It can be further concluded that with cooling water velocities up to 9.0 ft/sec, the greatest resistance to heat transfer is on the cooling water side, and above this velocity the greatest resistance is on the steam side.

B. RECOMMENDATIONS

To reduce the uncertainty in the cooling water mass flow rate at low flow rates, it is recommended that a smaller rotameter be used at the low flow rates.

The Wilson Plot technique is necessary in determining the inside and outside heat transfer coefficients so that a determination can be made as to the largest resistance to heat transfer, particularly when studying new tubes. There appears to be inherent uncertainties in this technique, especially in the determination of the outside heat transfer coefficient where uncertainties are in the order of 15 percent [4]. Because of these uncertainties it is recommended that a corrected overall heat transfer coefficient be used for design purposes, thus reducing uncertainty. As defined by the Heat Transfer Research, Inc., the corrected overall heat transfer coefficient is the experimentally obtained overall heat transfer coefficient less the wall resistance.

The following tests are recommended:

1. Experimentally test various tube geometries under the following conditions:
    a. various cooling water velocities
    b. various degrees of fouling
    c. various steam velocities
    d. various test condenser pressures
    e. various percentages of non-condensable gases
    f. various amounts of inundation
2. After testing with a single tube, the testing should be expanded to test a bank of tubes under the same conditions as outlined above.

To increase the steam mass flow rate it is recommended that the house steam be connected to the existing system. With the incorporation of house steam, testing with various steam velocities will be possible.

TABLE I. Summary of Comparative Qualities of Some Enhanced Tubes [6].

| Tube Number | Tube Type | Pressure Drop Ratio $\bar{P} = \frac{\Delta P_r}{\Delta P_s}$ | Overall Coefficient Ratio $\bar{U} = \frac{U_r}{U_s}$ | Overall Performance Ratio (OPR) $= \frac{\bar{U}}{\bar{P}}$ | Tube Side Coefficient Ratio $\bar{h} = \frac{h_r}{h_s}$ | Tube Side Performance Ratio (TPR) $= \frac{\bar{h}}{\bar{P}}$ |
|---|---|---|---|---|---|---|
| S. 3 | a | 4.54 | 1.690 | 0.372 | 1.788 | 0.394 |
| S.12 | a | 2.00 | 1.456 | 0.728 | 1.357 | 0.678 |
| S.13 | a | 1.50 | 1.541 | 1.027 | 1.203 | 0.802 |
| S.14 | a | 1.318 | 1.544 | 1.171 | 1.116 | 0.847 |
| S.17 | a | 6.970 | 1.988 | 0.285 | 2.212 | 0.317 |
| RM 41 | (b) | 2.273 | 1.755 | 0.772 | 1.232 | 0.542 |
| S.43 | a | 2.045 | 1.399 | 0.684 | 1.556 | 0.761 |
| S.44 | a | 3.485 | 1.554 | 0.446 | 1.659 | 0.476 |
| S.46 | a | 7.227 | 1.904 | 0.264 | 2.476 | 0.343 |
| S. 4 | c | 3.088 | 1.821 | 0.590 | 1.472 | 0.477 |
| S. 7 | c | 4.382 | 2.023 | 0.462 | 1.902 | 0.434 |
| S. 9 | c | 3.559 | 1.905 | 0.535 | 1.675 | 0.471 |
| S.10 | c | 1.794 | 1.702 | 0.949 | 1.258 | 0.701 |
| S.11 | c | 1.66 | 1.607 | 0.968 | 1.193 | 0.718 |
| S.16 | c | 1.787 | 1.565 | 0.876 | 1.264 | 0.707 |
| S.8 | d | 5.97 | 2.109 | 0.353 | 2.129 | 0.357 |
| G. 6 | e | 2.103 | 1.798 | 0.855 | 1.315 | 0.625 |
| G.30 | e | 2.152 | 1.926 | 0.895 | 1.466 | 0.681 |
| G.31 | e | 1.909 | 1.868 | 0.978 | 1.338 | 0.701 |
| G.32 | e | 2.515 | 2.036 | 0.809 | 1.659 | 0.766 |
| G.33 | e | 1.742 | 1.904 | 1.091 | 1.228 | 0.705 |
| G.35 | f | 2.030 | 1.846 | 0.909 | 1.370 | 0.675 |
| G.36 | f | 2.030 | 1.736 | 0.855 | 1.337 | 0.659 |
| G.47 | f | 1.470 | 1.609 | 1.094 | 1.190 | 0.586 |

TABLE II. Test Run Description

| Run | Preparation | Condensation Mode |
|---|---|---|
| 1(Aug 6) | None | Mixed dropwise and filmwise |
| 2(Aug 7) | None | Mixed dropwise and filmwise |
| 3(Aug 12) | Outside Treatment | Pure filmwise, some fouling |
| 4(Aug 14) | Outside Treatment | Pure filmwise, some fouling |
| 5(Aug 18) | Outside and Inside Treatment | Pure filmwise, clean |

TABLE III. Pressure Drop Results

| | | Isothermal | | Non-Isothermal | |
|---|---|---|---|---|---|
| Flow Rate | Run | Reynolds Number | Friction Factor | Reynolds Number | Friction Factor |
| 20 | 1,2,5 | 25920 | 0.0071 ± 0.0009 | 27104 | 0.0066 ± 0.0008 |
| | 3,4 | 25920 | 0.0071 ± 0.0009 | 26671 | 0.0062 ± 0.0007 |
| 30 | 1,2,5 | 39273 | 0.0059 ± 0.0005 | 40533 | 0.0057 ± 0.0003 |
| | 3,4 | 39273 | 0.0059 ± 0.0005 | 39839 | 0.0054 ± 0.0003 |
| 40 | 1,2,5 | 52576 | 0.0055 ± 0.0003 | 54001 | 0.0053 ± 0.0002 |
| | 3,4 | 52576 | 0.0057 ± 0.0003 | 53804 | 0.0052 ± 0.0002 |
| 50 | 1,2,5 | 64609 | 0.0053 ± 0.0002 | 66354 | 0.0055 ± 0.0003 |
| | 3,4 | 64609 | 0.0055 ± 0.0002 | 64293 | 0.0051 ± 0.0002 |
| 60 | 1,2,5 | 77105 | 0.0052 ± 0.0002 | 78781 | 0.0052 ± 0.0002 |
| | 3,4 | 77105 | 0.0053 ± 0.0002 | 77093 | 0.0049 ± 0.0002 |
| 70 | 1,2,5 | 90099 | 0.0050 ± 0.0002 | 92078 | 0.0051 ± 0.0002 |
| | 3,4 | 90099 | 0.0051 ± 0.0002 | 89689 | 0.0048 ± 0.0002 |
| 80 | 1,2,5 | 102641 | 0.0049 ± 0.0001 | 103875 | 0.0050 ± 0.0001 |
| | 3,4 | 102641 | 0.0050 ± 0.0001 | 101682 | 0.0047 ± 0.0001 |
| 90 | 1,2,5 | 115907 | 0.0047 ± 0.0001 | 116187 | 0.0047 ± 0.0001 |
| | 3,4 | 115907 | 0.0049 ± 0.0001 | 114291 | 0.0046 ± 0.0001 |

TABLE IV. Heat Transfer Results

| Flow Rate % | Run | Velocity ft/sec | Vapor Temp °F | Cooling Water Inlet Temp °F | Overall Heat Transfer Coefficient BTU/hr-ft²-°F | $C_1$ | Inside Heat Transfer Coefficient BTU/hr-ft²-°F | Outside Heat Transfer Coefficient BTU/hr-ft²-°F | Reynolds Number | Isothermal Pressure Drop " Hg | Non-Isothermal Pressure Drop " Hg |
|---|---|---|---|---|---|---|---|---|---|---|---|
| 20 | 1 | 5.63 | 145.4 | 75.6 | 743 ± 48 | 0.0276 | 1502 ± 122 | 2603 ± 737 | 27014 | 1.35 | 1.2 |
| | 2 | 5.61 | 144.7 | 75.2 | 760 ± 49 | 0.0276 | 1497 ± 121 | 2841 ± 866 | 26882 | 1.3 | 1.2 |
| | 3 | 5.73 | 145.9 | 73.8 | 659 ± 43 | 0.0276 | 1521 ± 123 | 1840 ± 397 | 26671 | | 1.2 |
| | 4 | 5.51 | 145.6 | 74.5 | 669 ± 43 | 0.0276 | 1520 ± 123 | 1923 ± 431 | 26799 | 1.3 | 1.2 |
| | 5 | 5.62 | 144.0 | 76.3 | 720 ± 48 | 0.0282 | 1559 ± 126 | 2301 ± 587 | 27460 | 1.3 | 1.2 |
| 25 | 1 | 7.01 | 144.7 | 75.9 | 843 ± 50 | 0.0276 | 1804 ± 139 | 2788 ± 675 | 33603 | | 1.8 |
| | 2 | 7.01 | 144.9 | 74.8 | 842 ± 49 | 0.0276 | 1785 ± 137 | 2837 ± 692 | 33118 | | 1.8 |
| | 3 | 7.17 | 145.4 | 73.9 | 736 ± 44 | 0.0276 | 1805 ± 139 | 1963 ± 365 | 33023 | | 1.7 |
| | 4 | 7.17 | 145.4 | 73.9 | 736 ± 44 | 0.0276 | 1805 ± 139 | 1963 ± 438 | 33023 | | 1.7 |
| | 5 | 7.03 | 144.3 | 76.5 | 786 ± 47 | 0.0282 | 1858 ± 143 | 2260 ± 466 | 33989 | | 1.8 |
| 30 | 1 | 8.50 | 144.5 | 76.1 | 897 ± 50 | 0.0276 | 2091 ± 157 | 2654 ± 533 | 40533 | 2.60 | 2.4 |
| | 2 | 8.49 | 145.0 | 74.5 | 916 ± 50 | 0.0276 | 2085 ± 156 | 2839 ± 596 | 39951 | 2.60 | 2.4 |
| | 3 | 8.69 | 145.8 | 74.1 | 805 ± 45 | 0.0276 | 2103 ± 158 | 2050 ± 342 | 39839 | | 2.4 |
| | 4 | 8.69 | 145.4 | 73.8 | 787 ± 45 | 0.0276 | 2101 ± 158 | 1940 ± 314 | 39652 | 2.6 | 2.4 |
| | 5a | 8.69 | 144.3 | 76.5 | 885 ± 50 | 0.0282 | 2166 ± 162 | 2548 ± 499 | 41199 | 2.6 | 2.4 |
| | 5b | 8.69 | 144.3 | 75.9 | 886 ± 50 | 0.0282 | 2166 ± 162 | 2561 ± 497 | 40999 | 2.6 | 2.4 |
| 40 | 1 | 11.37 | 144.3 | 76.5 | 1012 ± 56 | 0.0276 | 2625 ± 192 | 2738 ± 531 | 54001 | 4.3 | 4.0 |
| | 2 | 11.37 | 144.7 | 74.5 | 1051 ± 56 | 0.0276 | 2617 ± 191 | 3059 ± 566 | 52997 | 4.3 | 4.0 |
| | 3 | 11.63 | 145.6 | 74.5 | 875 ± 49 | 0.0276 | 2654 ± 194 | 1971 ± 280 | 53084 | | 4.0 |
| | 4 | 11.63 | 145.8 | 73.4 | 870 ± 48 | 0.0276 | 2634 ± 192 | 1962 ± 275 | 52347 | 4.4 | 4.1 |
| | 5 | 11.64 | 144.3 | 76.6 | 987 ± 54 | 0.0282 | 2719 ± 198 | 2576 ± 428 | 54623 | 4.3 | 4.0 |
| 50 | 1 | 13.97 | 144.3 | 76.8 | 1088 ± 61 | 0.0276 | 3056 ± 220 | 2778 ± 453 | 66354 | 6.3 | 6.0 |
| | 2 | 13.97 | 144.5 | 76.1 | 1104 ± 61 | 0.0276 | 3090 ± 222 | 2776 ± 441 | 64485 | 6.4 | 6.1 |
| | 3 | 14.29 | 145.9 | 74.7 | 908 ± 53 | 0.0276 | 3126 ± 225 | 1874 ± 247 | 64923 | | 6.0 |
| | 4 | 14.29 | 144.2 | 73.8 | 904 ± 54 | 0.0276 | 3121 ± 225 | 1859 ± 245 | 64025 | 6.5 | 6.1 |
| | 5a | 14.30 | 144.5 | 76.8 | 1037 ± 59 | 0.0282 | 3211 ± 231 | 2453 ± 368 | 67118 | 6.4 | 5.9 |
| | 5b | 14.30 | 144.3 | 75.7 | 1022 ± 58 | 0.0282 | 3188 ± 230 | 2392 ± 354 | 66159 | 6.4 | 5.9 |

| Flow Rate % | Run | Velocity ft/sec | Vapor Temp °F | Cooling Water Inlet Temp °F | Overall Heat Transfer Coefficient BTU/hr-ft²-°F | $C_i$ | Inside Heat Transfer Coefficient BTU/hr-ft²-°F | Outside Heat Transfer Coefficient BTU/hr-ft²-°F | Reynolds Number | Isothermal Pressure Drop " Hg | Non-Isothermal Pressure Drop " Hg |
|---|---|---|---|---|---|---|---|---|---|---|---|
| 60 | 1 | 16.67 | 144.1 | 77.0 | 1134 ± 67 | 0.0276 | 3541 ± 255 | 2659 ± 407 | 78781 | 8.8 | 8.2 |
| | 2 | 16.67 | 144.7 | 74.8 | 1159 ± 65 | 0.0276 | 3531 ± 254 | 2808 ± 427 | 76931 | 8.8 | 8.3 |
| | 3 | 17.05 | 145.8 | 74.7 | 961 ± 59 | 0.0276 | 3589 ± 258 | 1916 ± 253 | 77093 | | 8.3 |
| | 4 | 17.05 | 144.9 | 73.6 | 941 ± 59 | 0.0276 | 3568 ± 257 | 1842 ± 241 | 76033 | 9.0 | 8.6 |
| | 5 | 17.06 | 144.3 | 77 | 1056 ± 64 | 0.0282 | 3687 ± 265 | 2284 ± 324 | 79688 | 8.8 | 8.3 |
| 70 | 1 | 19.49 | 144.0 | 77 | 1218 ± 74 | 0.0276 | 3984 ± 283 | 2838 ± 440 | 92078 | 11.6 | 10.8 |
| | 2 | 19.48 | 144.5 | 75.6 | 1161 ± 72 | 0.0276 | 3973 ± 282 | 2554 ± 375 | 89917 | 11.6 | 11.1 |
| | 3 | 19.93 | 145.8 | 74.7 | 1021 ± 66 | 0.0276 | 4050 ± 288 | 1998 ± 268 | 89689 | | 11.1 |
| | 4 | 19.92 | 144.9 | 73.4 | 975 ± 65 | 0.0276 | 4029 ± 286 | 1840 ± 243 | 88058 | 11.8 | 11.4 |
| | 5a | 19.94 | 144.5 | 77 | 1164 ± 73 | 0.0282 | 4021 ± 285 | 2578 ± 384 | 92693 | 11.6 | 10.9 |
| | 5b | 19.93 | 144.3 | 75.9 | 1063 ± 70 | 0.0282 | 4003 ± 284 | 2135 ± 299 | 91381 | 11.6 | 10.9 |
| 80 | 1 | 22.19 | 144.0 | 76.6 | 1254 ± 82 | 0.0276 | 4375 ± 311 | 2818 ± 440 | 103875 | 14.6 | 13.8 |
| | 2 | 22.19 | 144.7 | 75.9 | 1203 ± 78 | 0.0276 | 4450 ± 316 | 2542 ± 371 | 102895 | 14.7 | 14.1 |
| | 3 | 22.70 | 145.8 | 74.7 | 1024 ± 72 | 0.0276 | 4488 ± 319 | 1905 ± 261 | 101682 | | 14.1 |
| | 4 | 22.69 | 144.9 | 73.2 | 993 ± 71 | 0.0276 | 4458 ± 317 | 2343 ± 319 | 99841 | 15.0 | 14.4 |
| | 5 | 22.70 | 144.1 | 76.8 | 1158 ± 79 | 0.0282 | 4612 ± 327 | 2380 ± 350 | 105071 | 14.6 | 13.8 |
| 90 | 1 | 25.06 | 144.9 | 75.7 | 1378 ± 88 | 0.0276 | 4944 ± 351 | 3174 ± 498 | 116187 | 18.0 | 17.0 |
| | 2 | 25.06 | 144.7 | 76.1 | 1281 ± 87 | 0.0276 | 4944 ± 351 | 2709 ± 409 | 116187 | 18.0 | 17.2 |
| | 3 | 25.63 | 145.6 | 74.3 | 1128 ± 81 | 0.0276 | 4987 ± 354 | 1808 ± 280 | 114291 | | |
| | 4 | 25.62 | 145.2 | 73.2 | 1039 ± 80 | 0.0276 | 4902 ± 348 | 1874 ± 268 | 112232 | 18.5 | 17.6 |
| | 5a | 25.64 | 144.1 | 76.5 | 1219 ± 86 | 0.0282 | 5085 ± 361 | 2492 ± 376 | 118082 | 18.0 | 17.9 |
| | 5b | 25.63 | 144.5 | 75.9 | 1173 ± 74 | 0.0282 | 5062 ± 359 | 2319 ± 343 | 116974 | 18.0 | 17.1 |

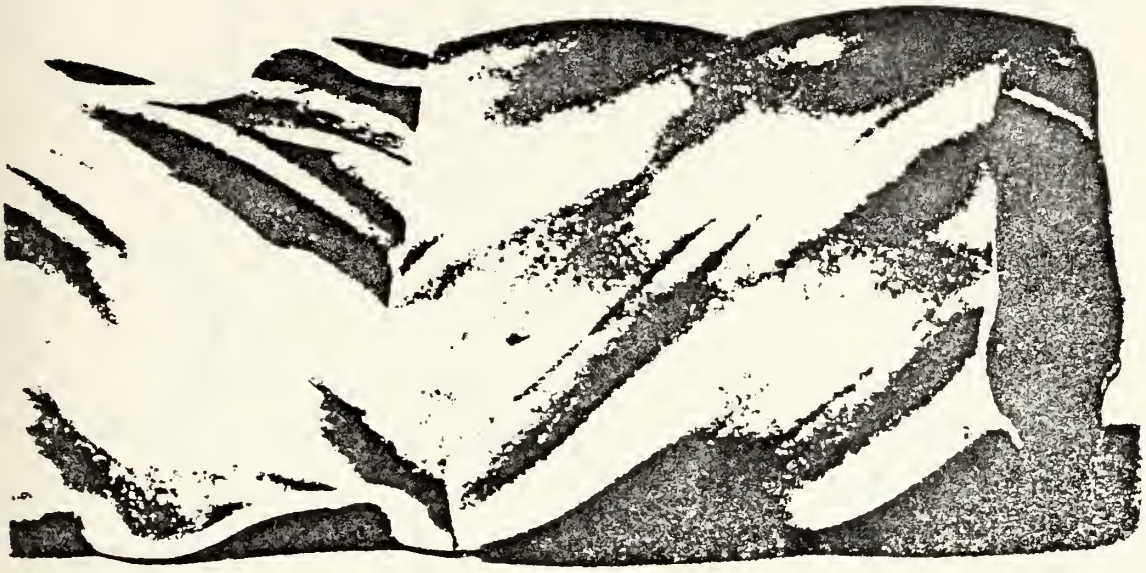

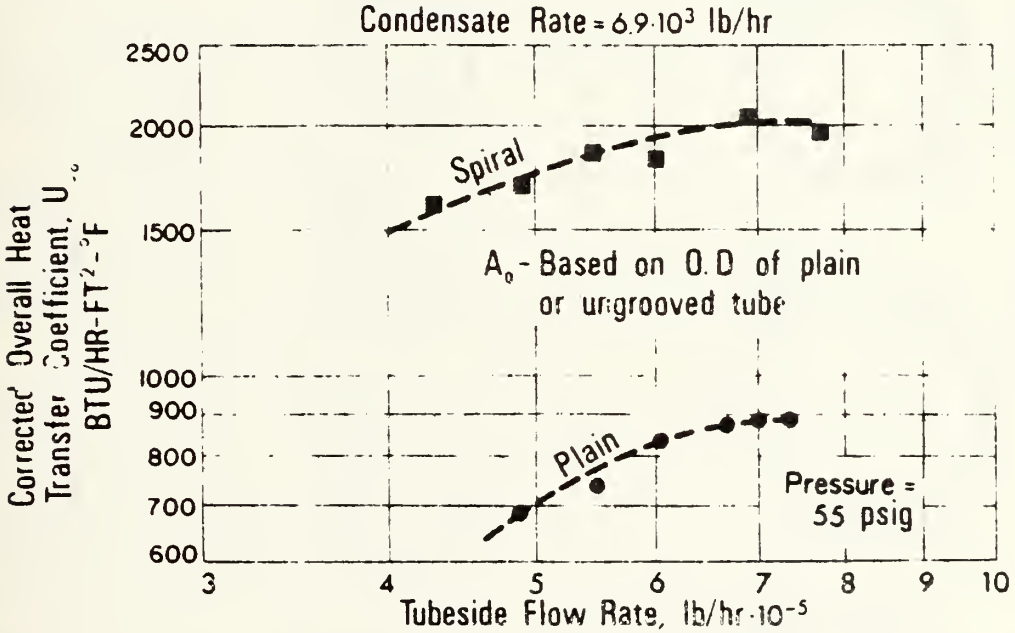


Figure 1. Turbotec Spirally Grooved Tube [4].

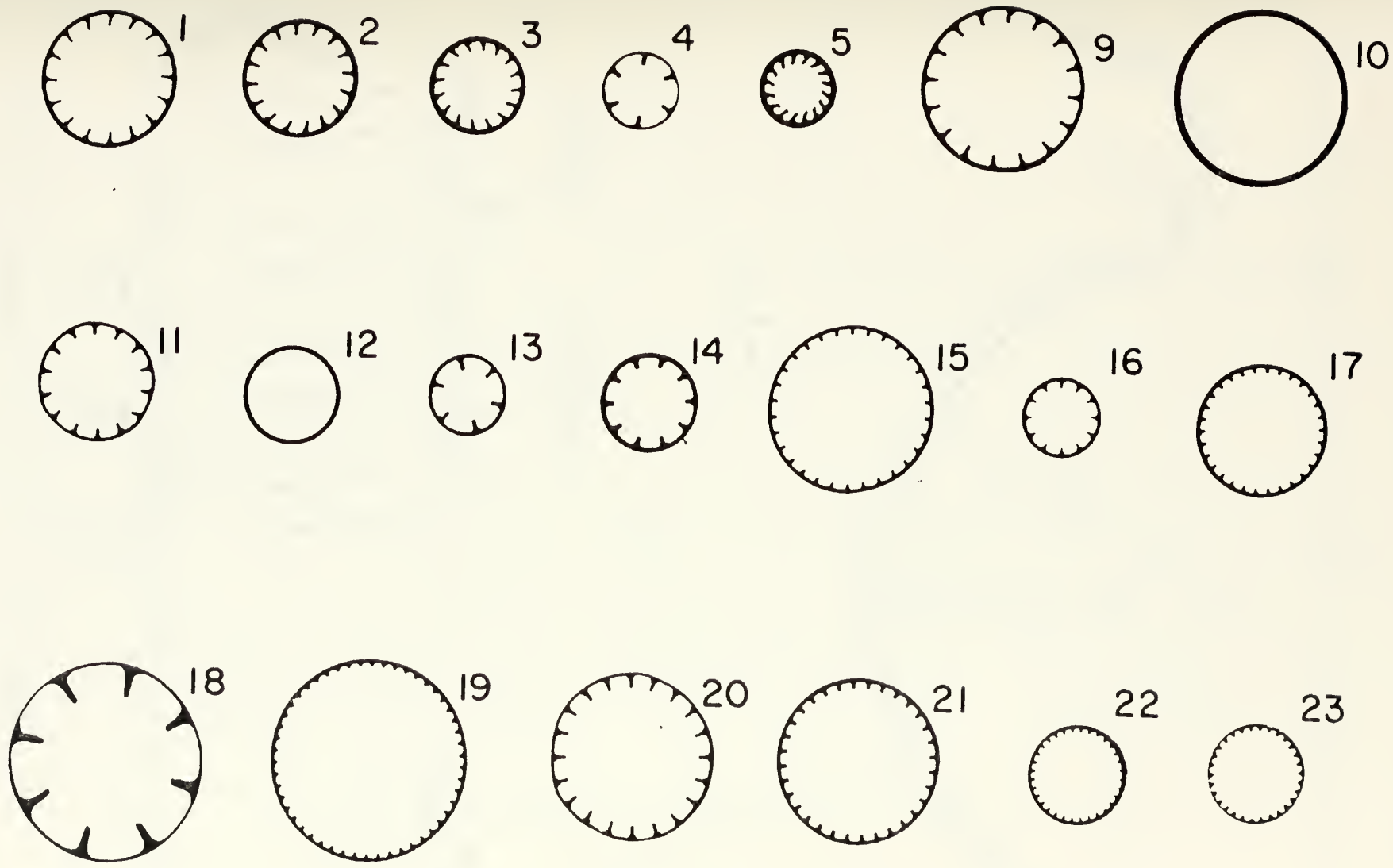


Figure 2. Cross-Section of Noranda Tubes [7].

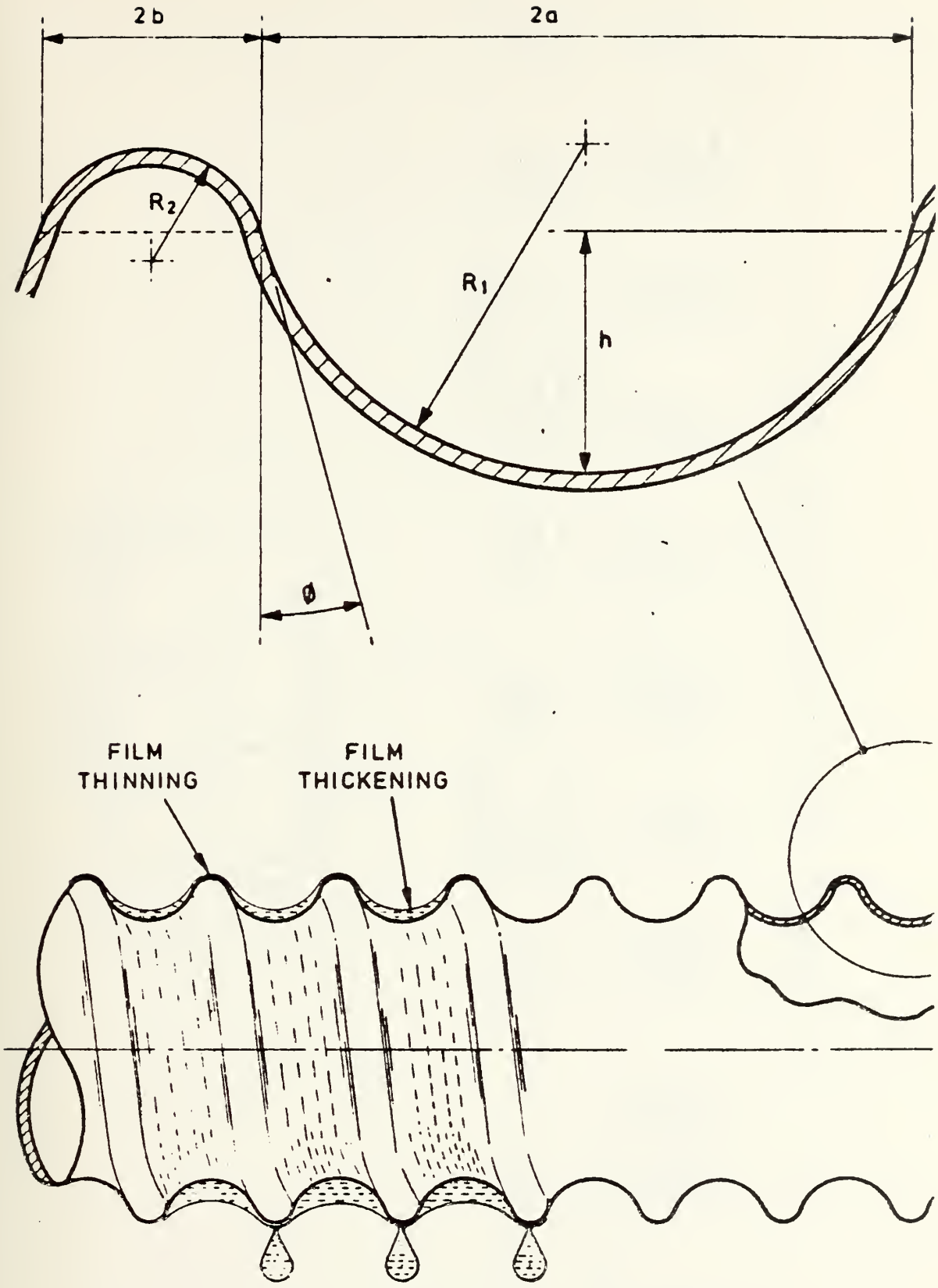


Figure 3. Catchpole and Drew's Test Tube (Kydensa)[8].

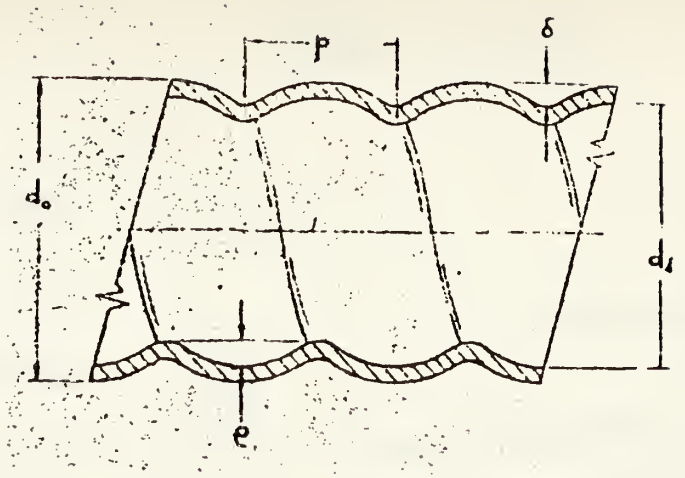


| Tube No. | Tube Material | Tube Interior: Inside Diameter $d_i$, in | Tube Interior: Inside Surface $A_i^*$, $ft^2/ft$ | Tube Interior: Ridge Height e, in | Tube Exterior: Outside Diameter $d_o$, in | Tube Exterior: Outside Surface $A_o^*$, $ft^2/ft$ | Tube Exterior: Groove Pitch p, in | Tube Exterior: Groove Depth $\delta$, in | Bank Layout Pitch |
|---|---|---|---|---|---|---|---|---|---|
| I | DHP copper | 0.530 | 0.139 | 0.0294 | 0.613 | 0.160 | 0.253 | 0.0272 | 0.875 |
| II | 90-10 CuNi | 0.822 | 0.215 | 0.0290 | 0.936 | 0.245 | 0.250 | 0.0310 | 1.250 |
| III | 90-10 CuNi | 0.855 | 0.224 | 0.0313 | 0.937 | 0.245 | 0.374 | 0.0302 | 1.250 |
| IV | 90-10 CuNi | 0.863 | 0.226 | 0.0408 | 0.943 | 0.247 | 0.501 | 0.0388 | 1.250 |

Figure 4. Withers and Young's Corrugated Tube [9].

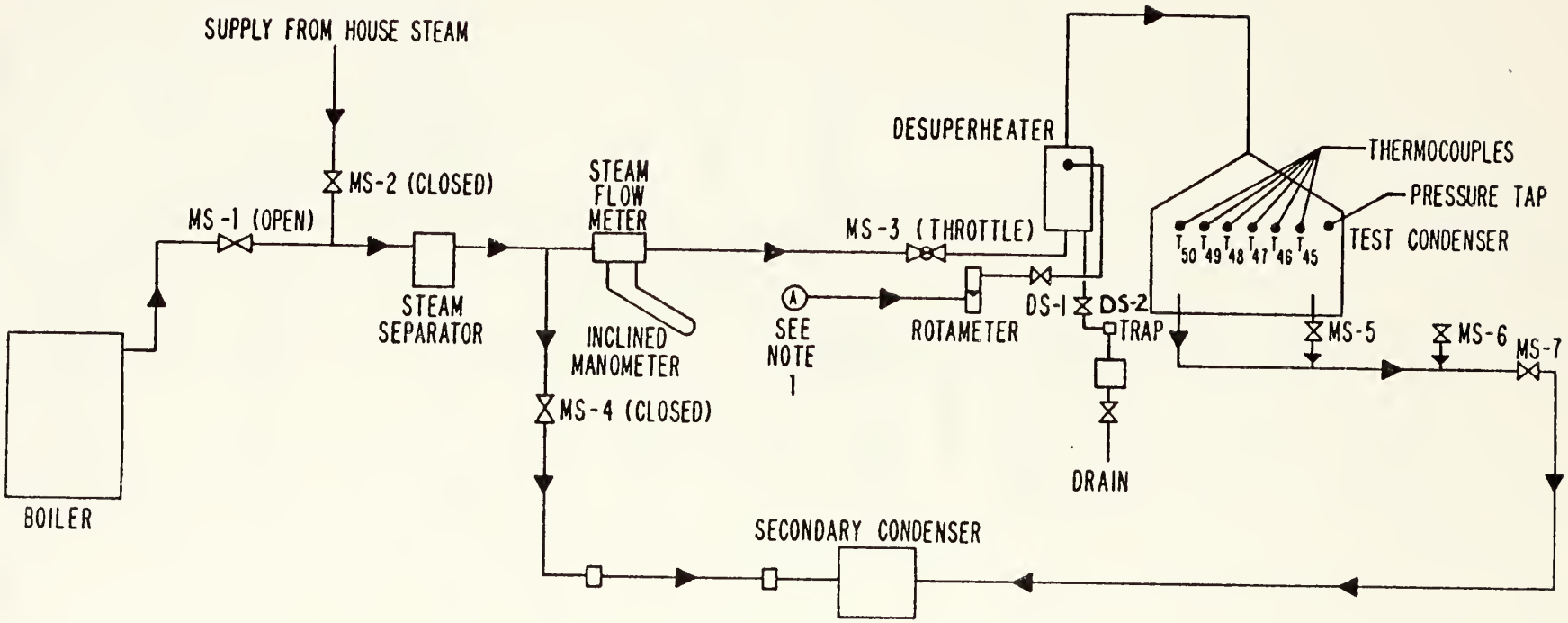


NOTE: From discharge of feed pump, see Figure 8.

Figure 5. Schematic of Steam System.

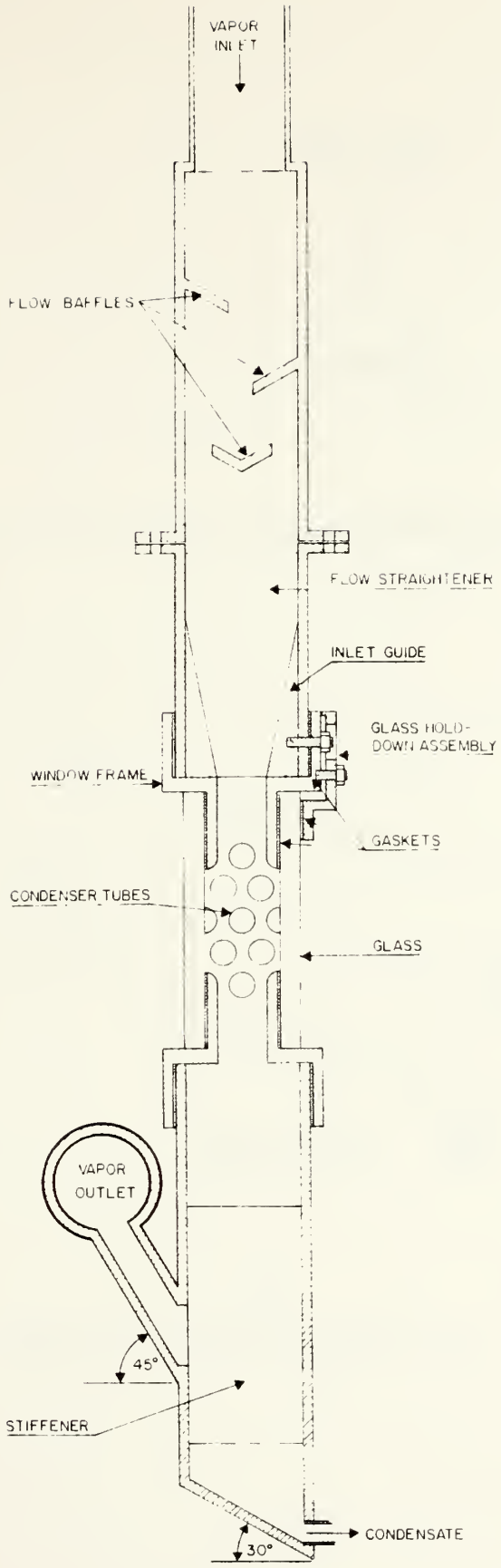


Figure 6. Test Condenser with Initial Tube Configuration.

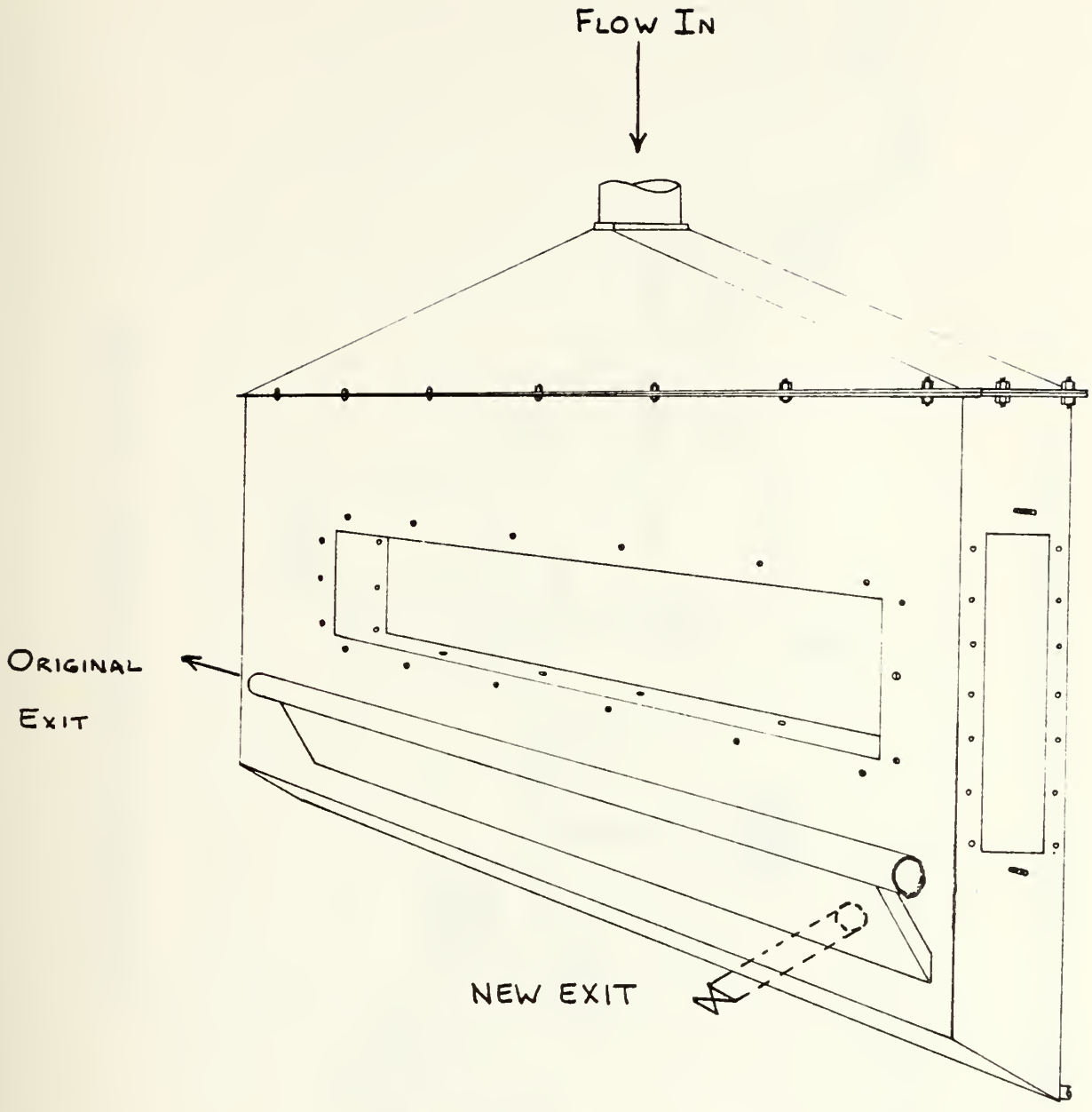


Figure 7. Schematic of Test Condenser Body.

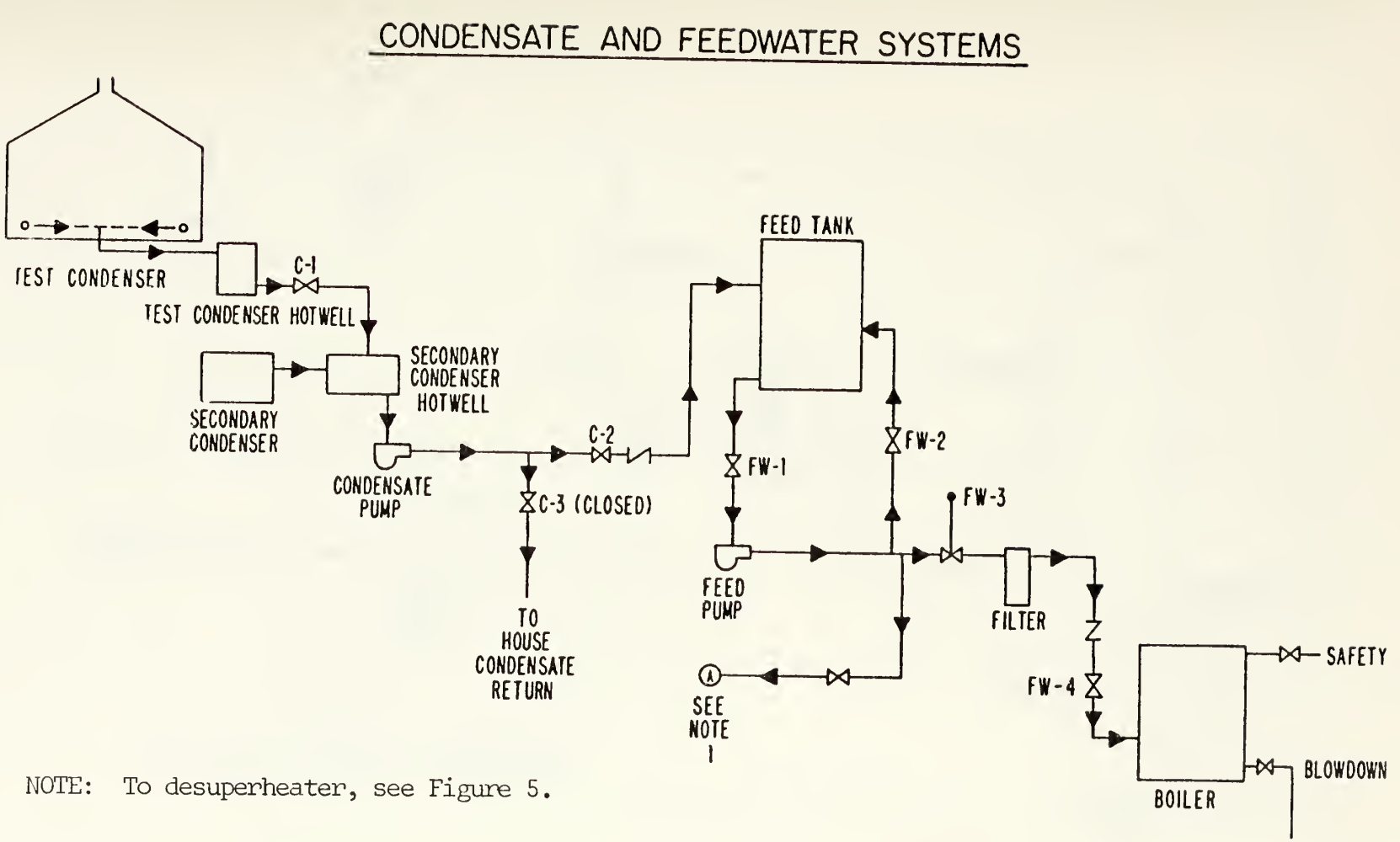


Figure 8. Schematic of Condensate and Feedwater System.

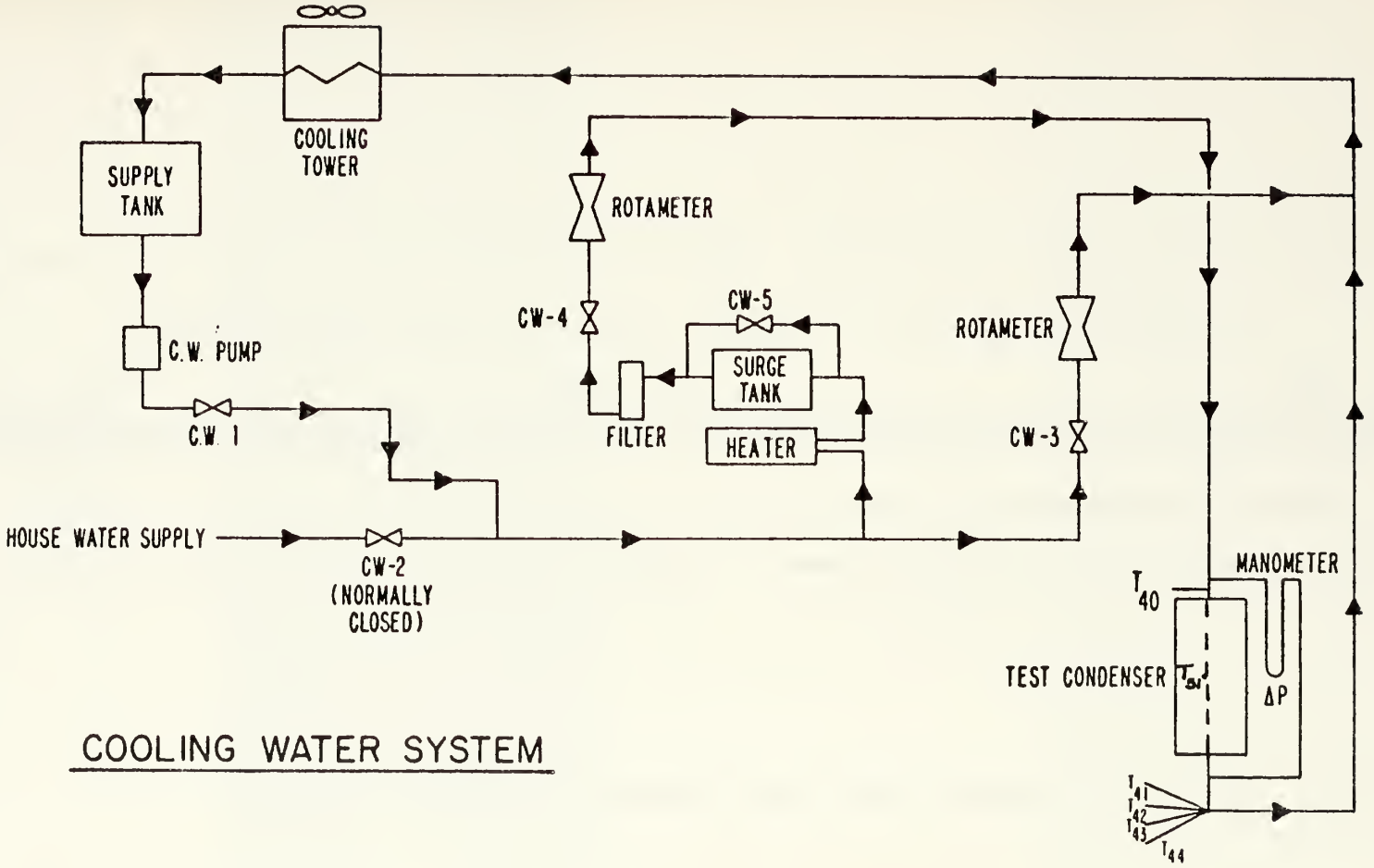


Figure 9. Schematic of Cooling Water System.

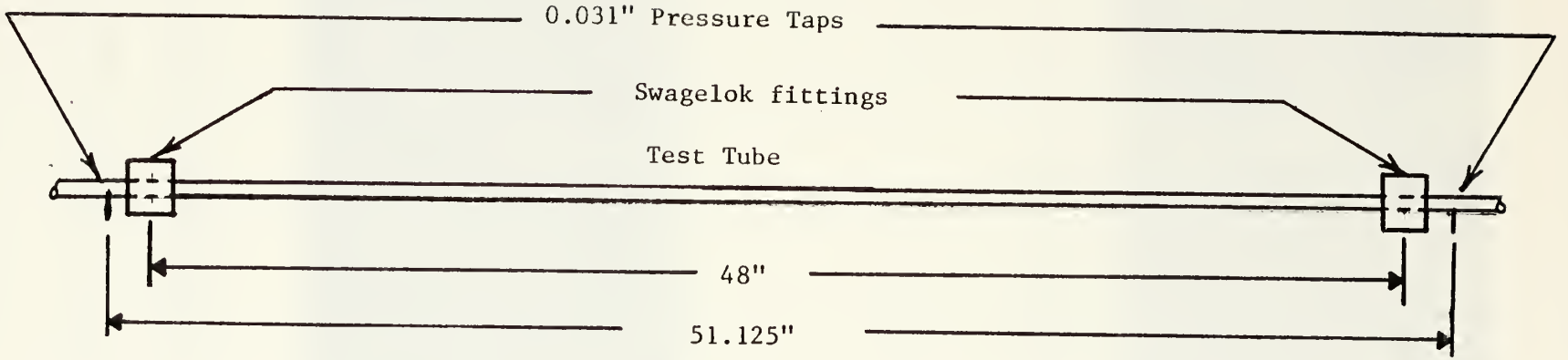


Figure 10. Schematic of Pressure Taps in Test Section.

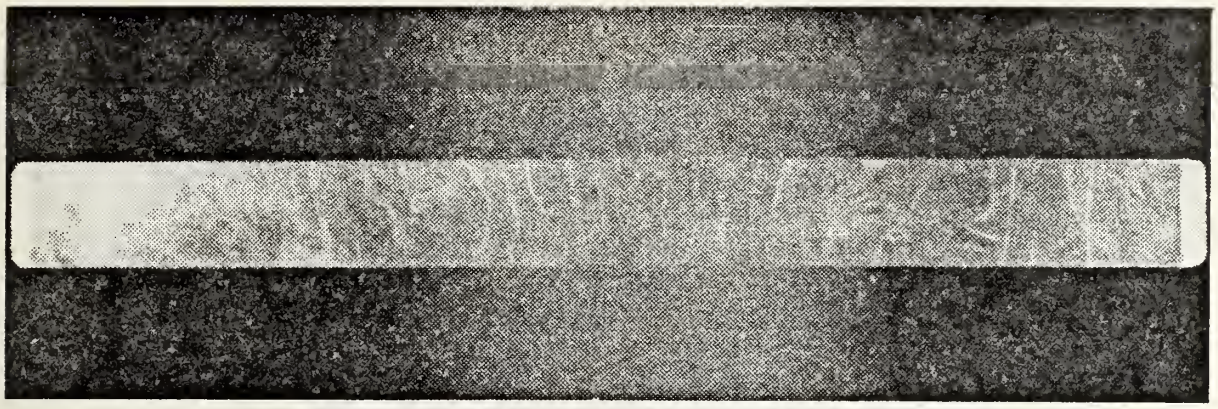

(a) Flow at low air velocities .

(b) Flow with smoke secured, showing stagnation regions.

Figure 11. Flow Visualization with Two Exits.

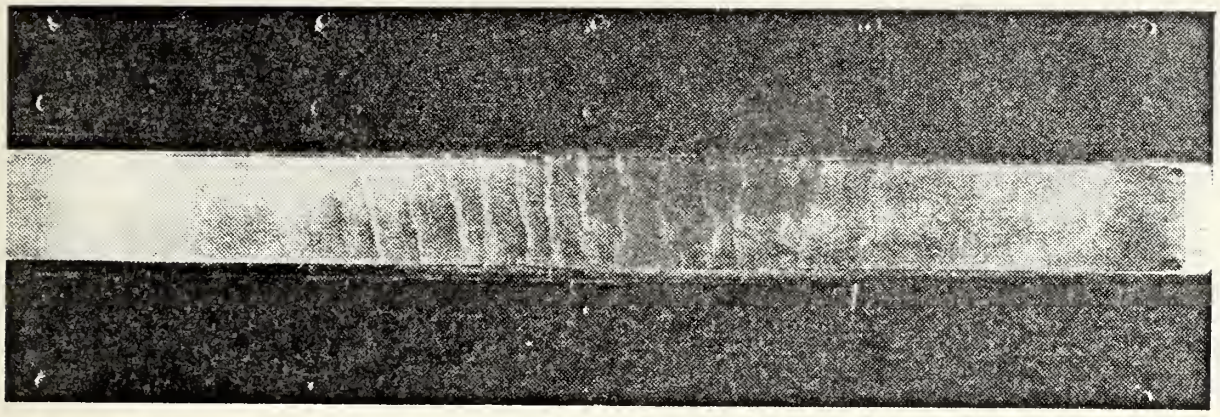

(a) Flow at low air velocities.

(b) Flow at high air velocities.

Figure 12. Flow Visualization with Two Exits Plus Inlet Screens.

(a) Valve open.

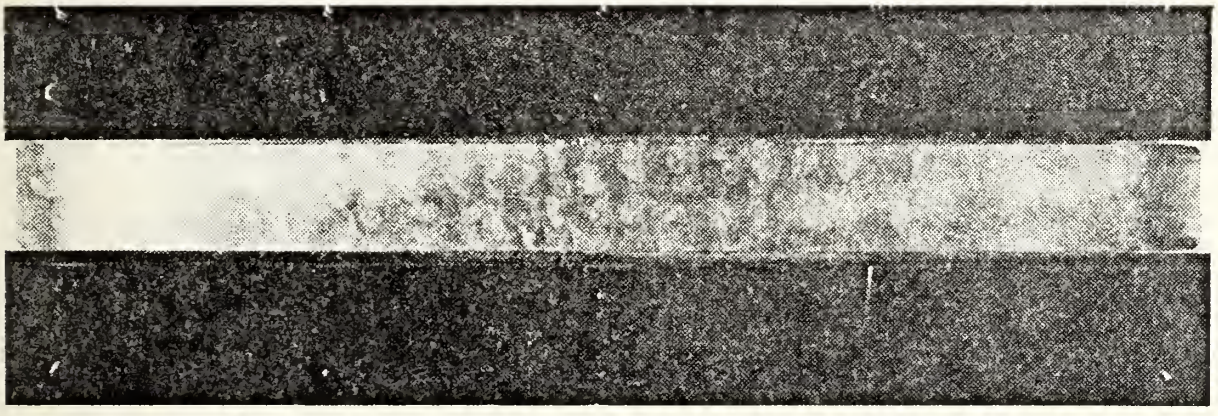

(b) Valve closed.

Figure 13. Comparison of Flow with Exit Valve Open and Closed.

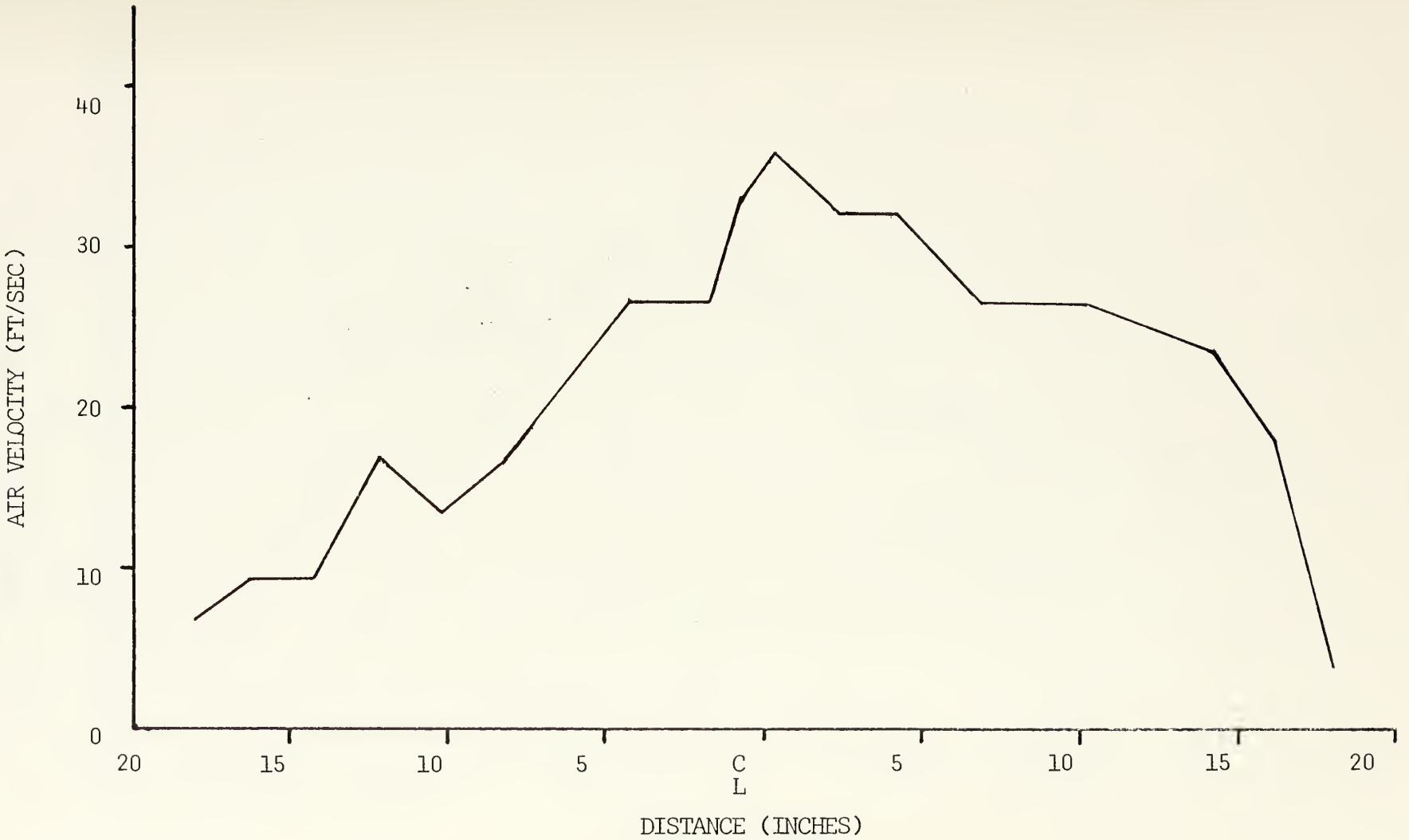


Figure 14. Velocity Profile with One Exit.

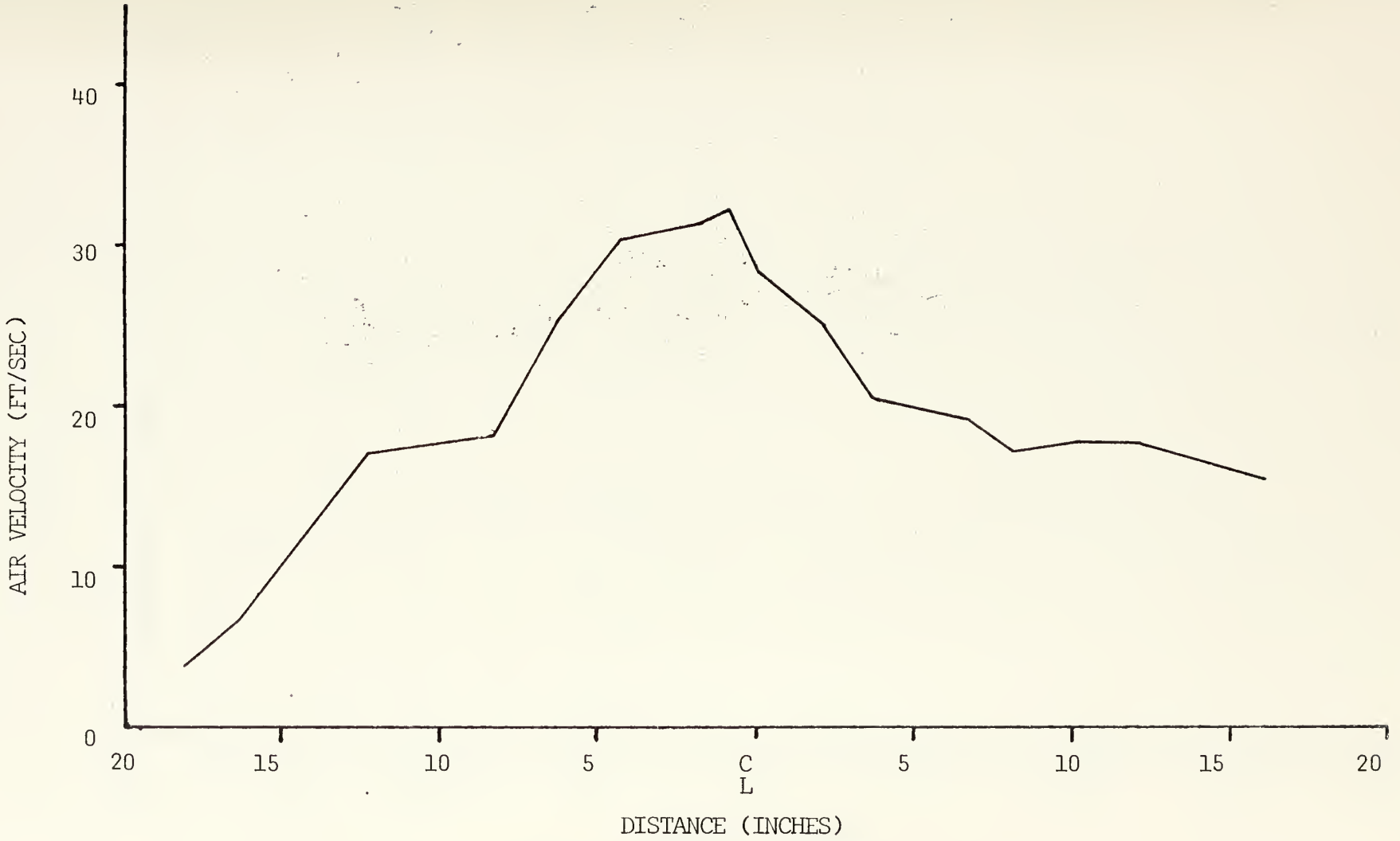


Figure 15. Velocity Profile with Two Exits.

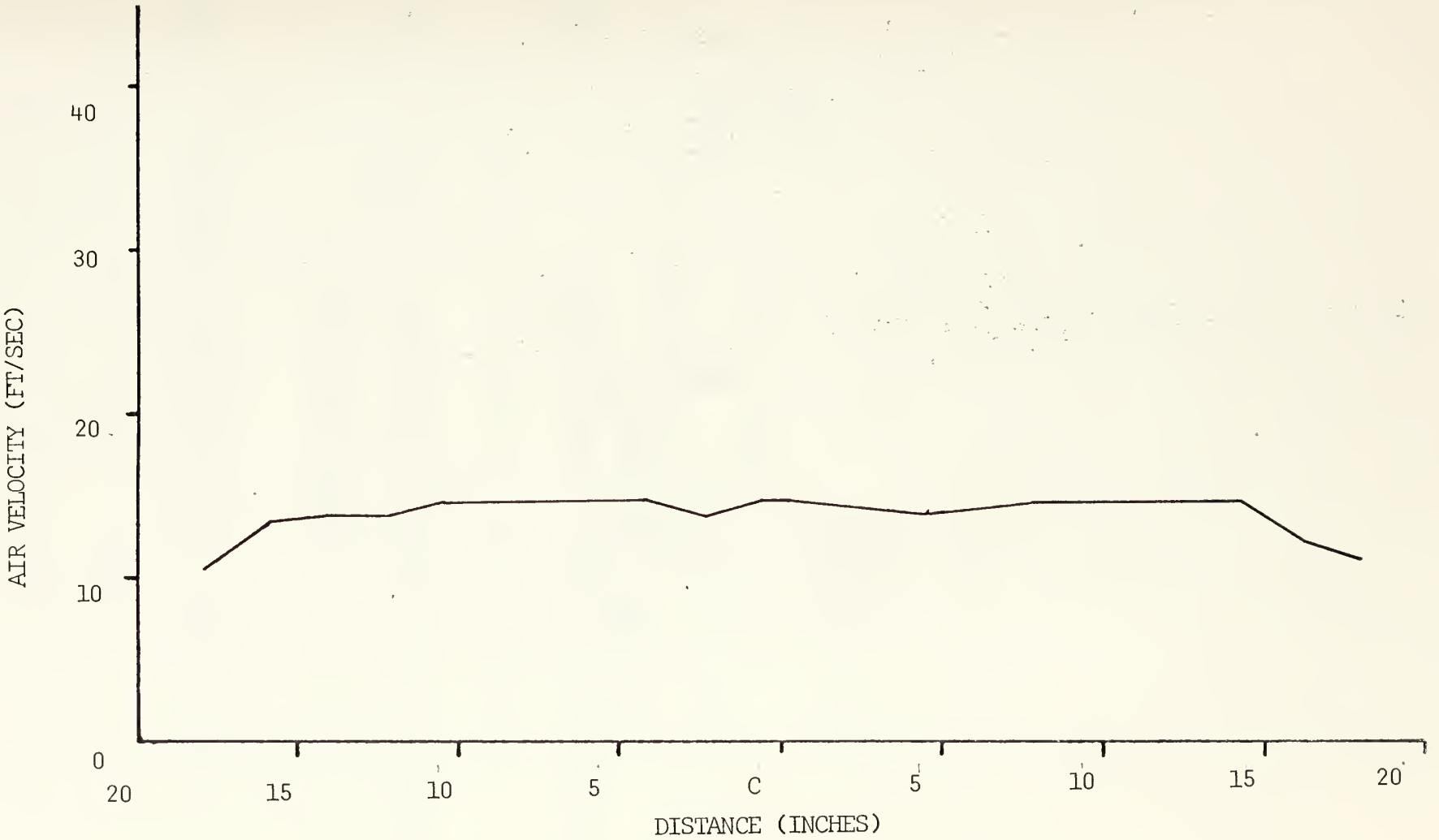


Figure 16. Velocity Profile with Two Exits and Inlet Screens.

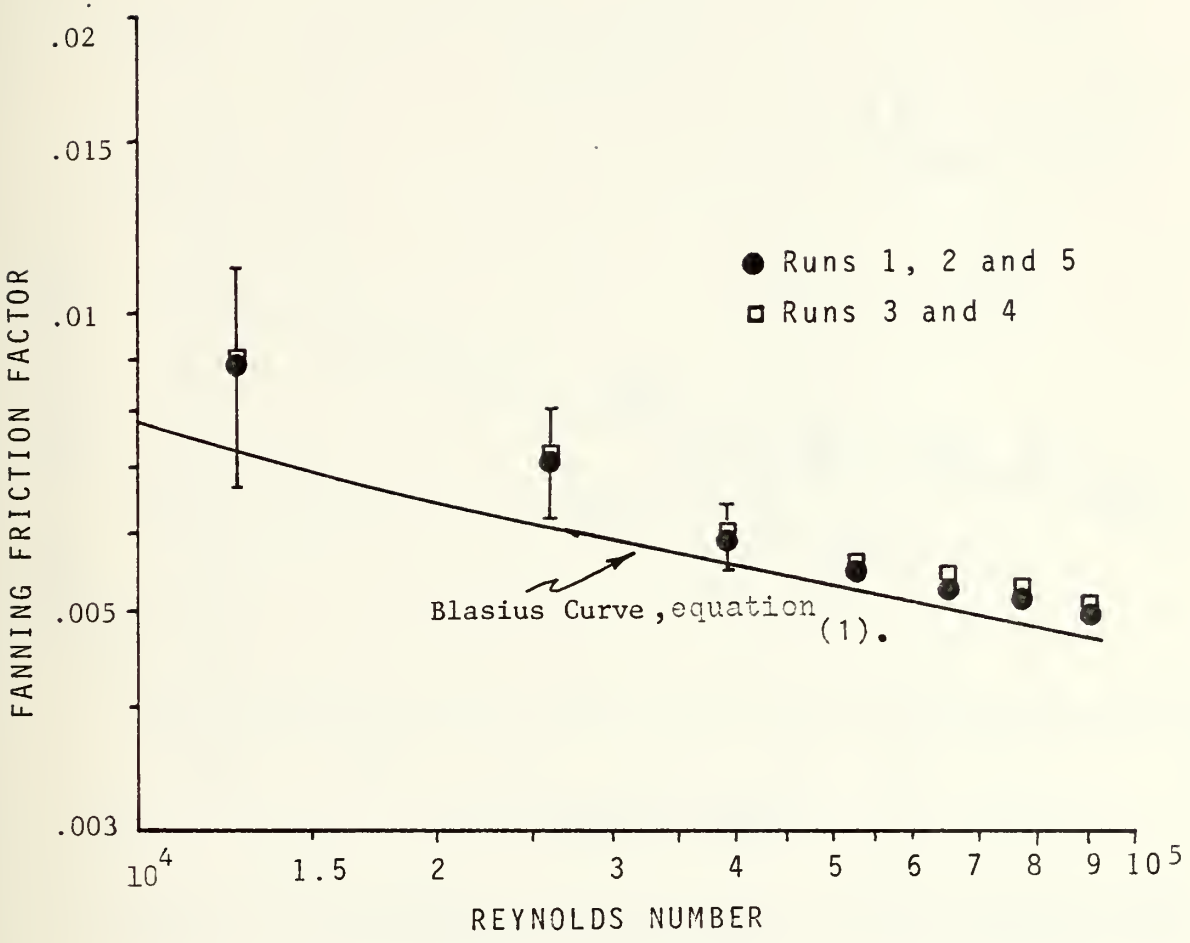


Figure 17. Isothermal Friction Factor Versus Reynolds Number.

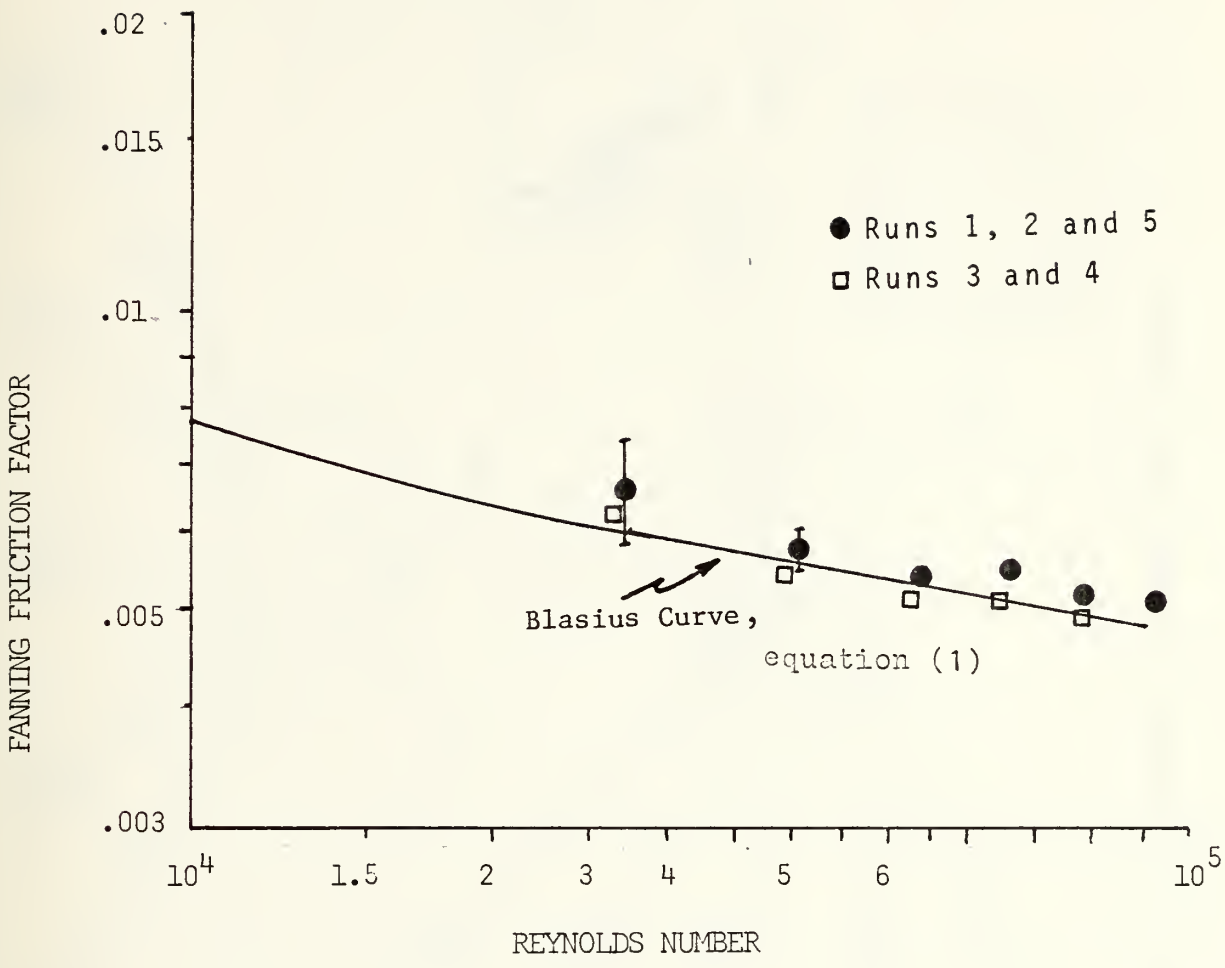


Figure 18. Non-Isothermal Friction Factor Versus Reynolds Number.

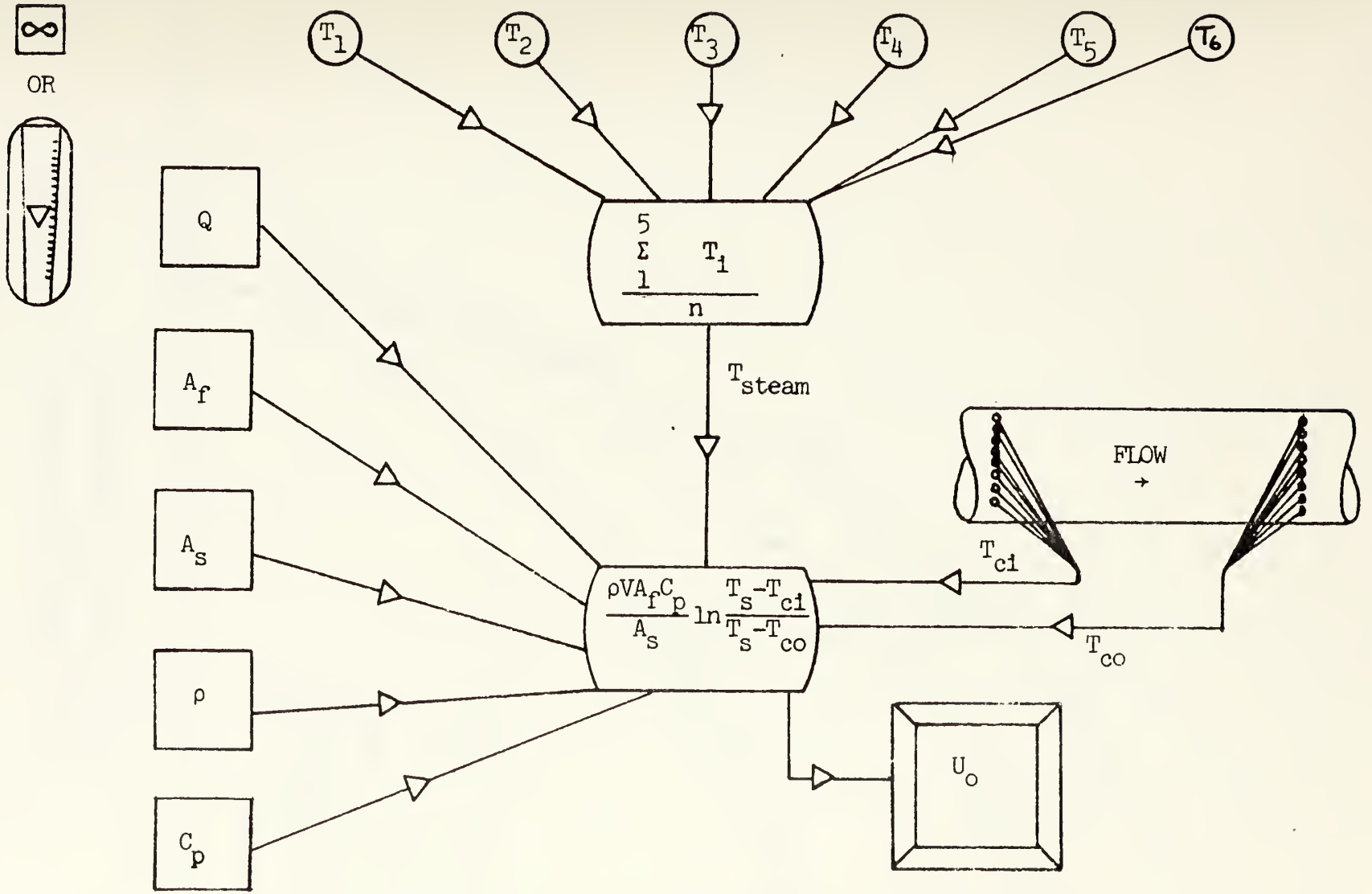


Figure 19. Schematic for Calculation of Overall Heat Transfer Coefficient, $U_o$.

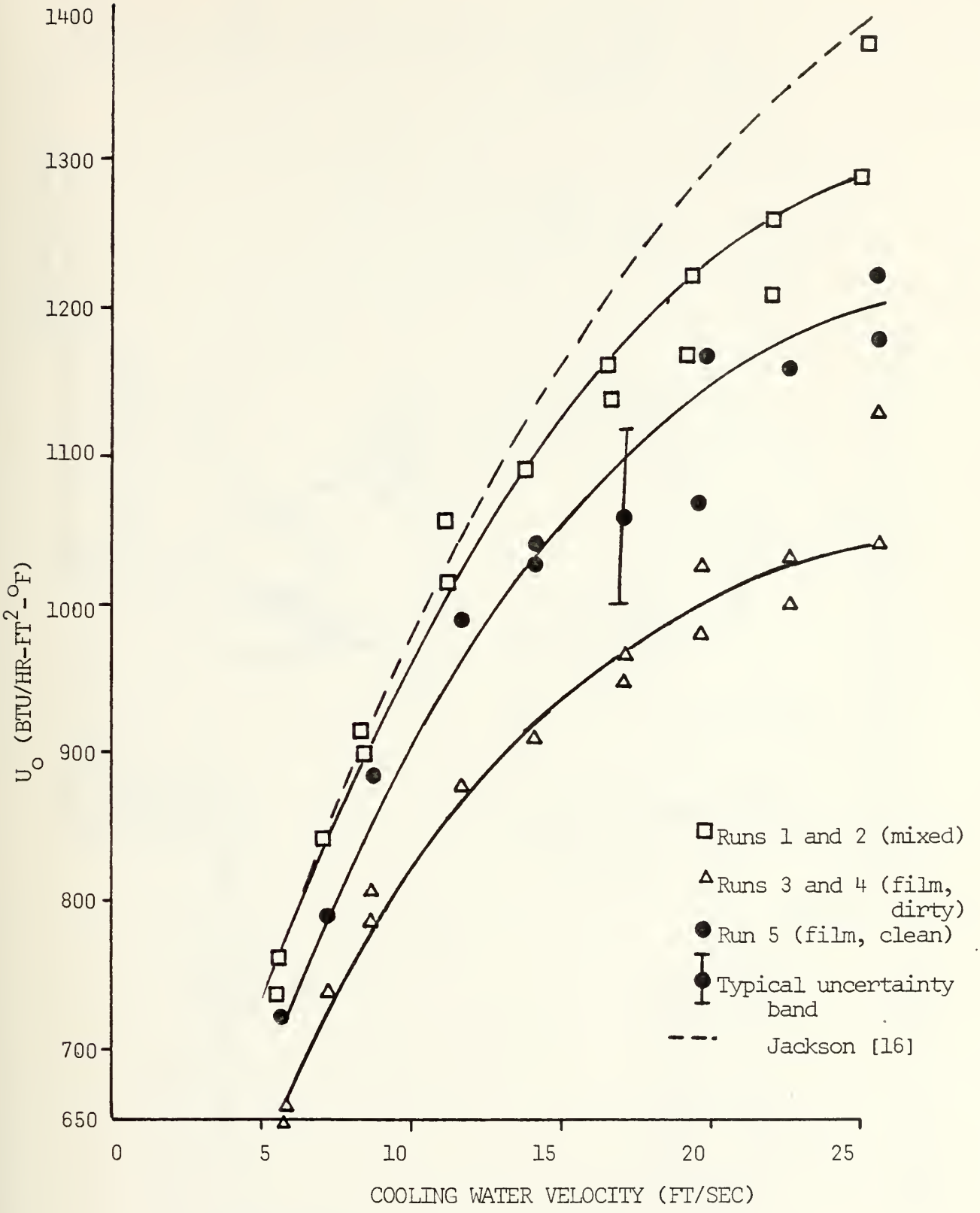


Figure 20. $U_o$ Versus Cooling Water Velocity.

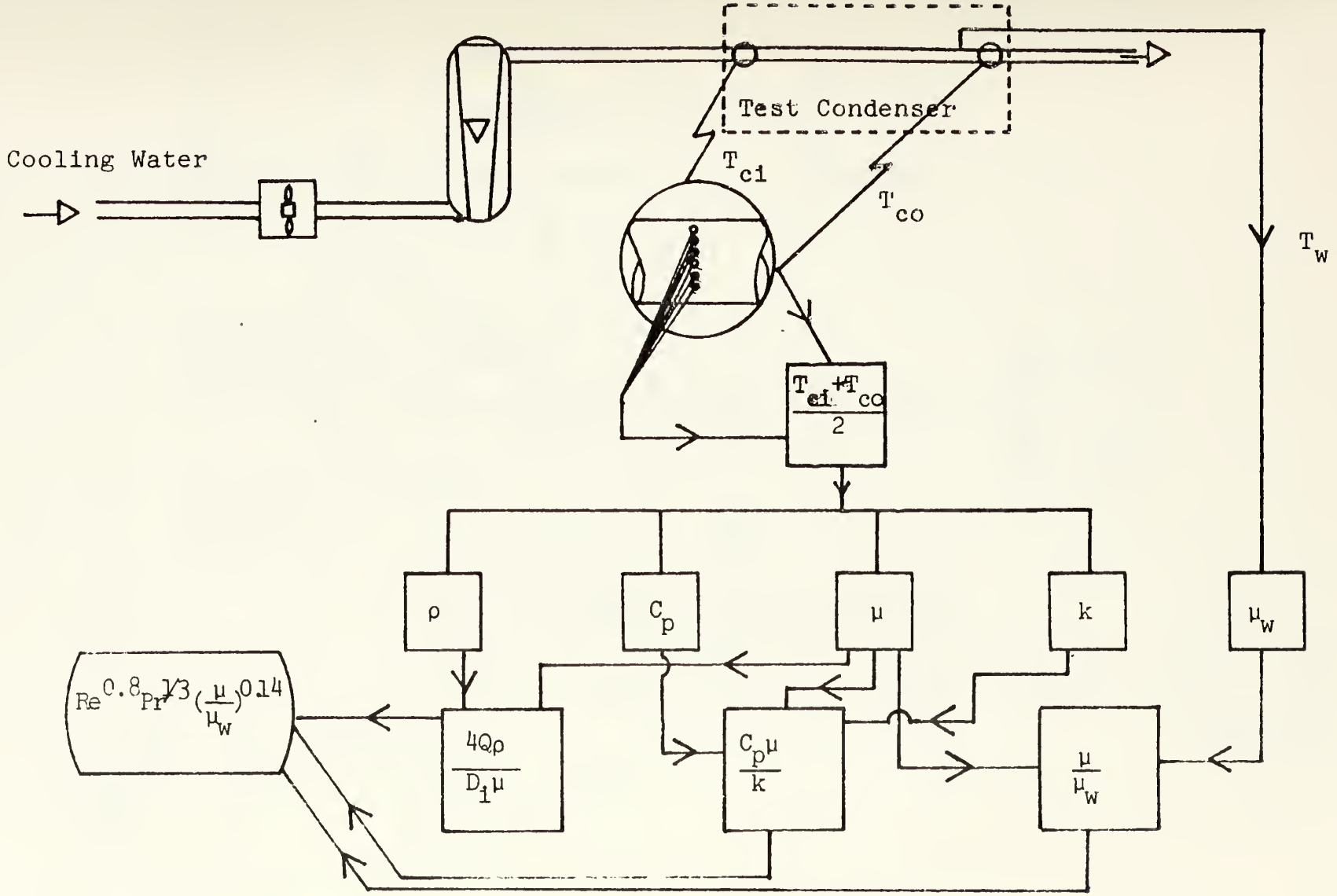


Figure 21. Schematic for Calculation of Inverse of Wilson Plot Abscissa.

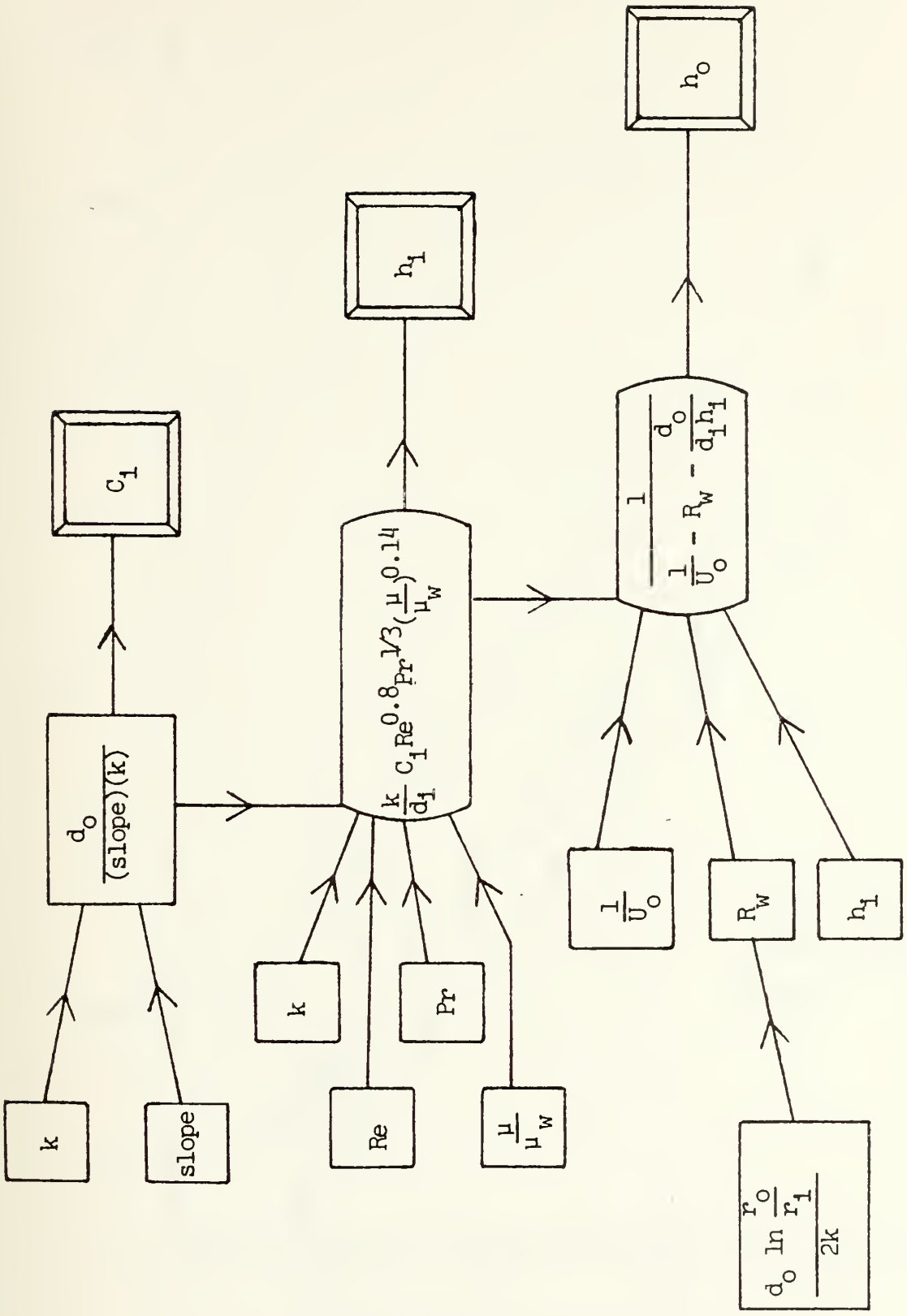


Figure 22. Schematic for Calculation of $C_i$; $h_i$, and $h_o$.

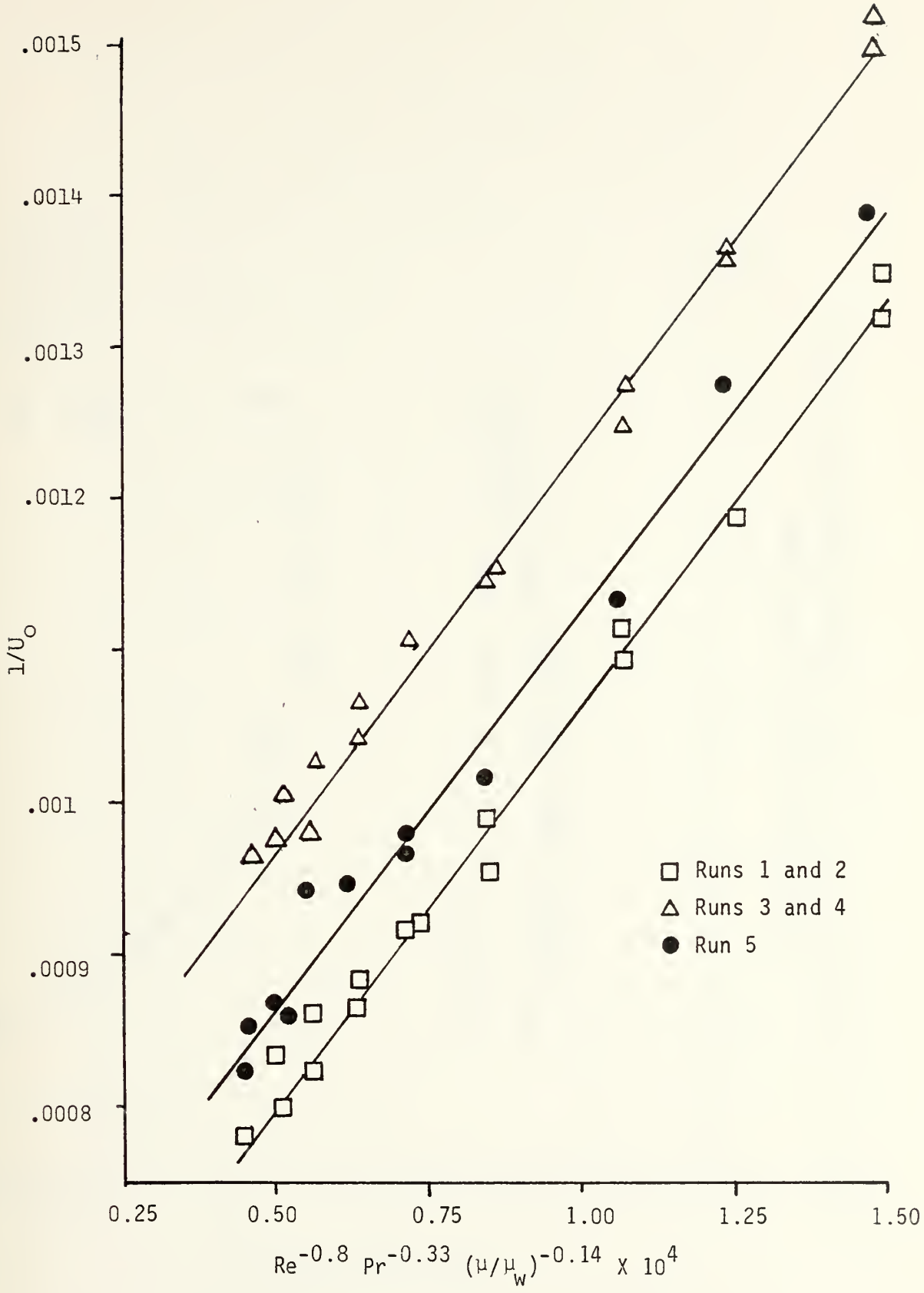


Figure 23. Modified Wilson Plot.

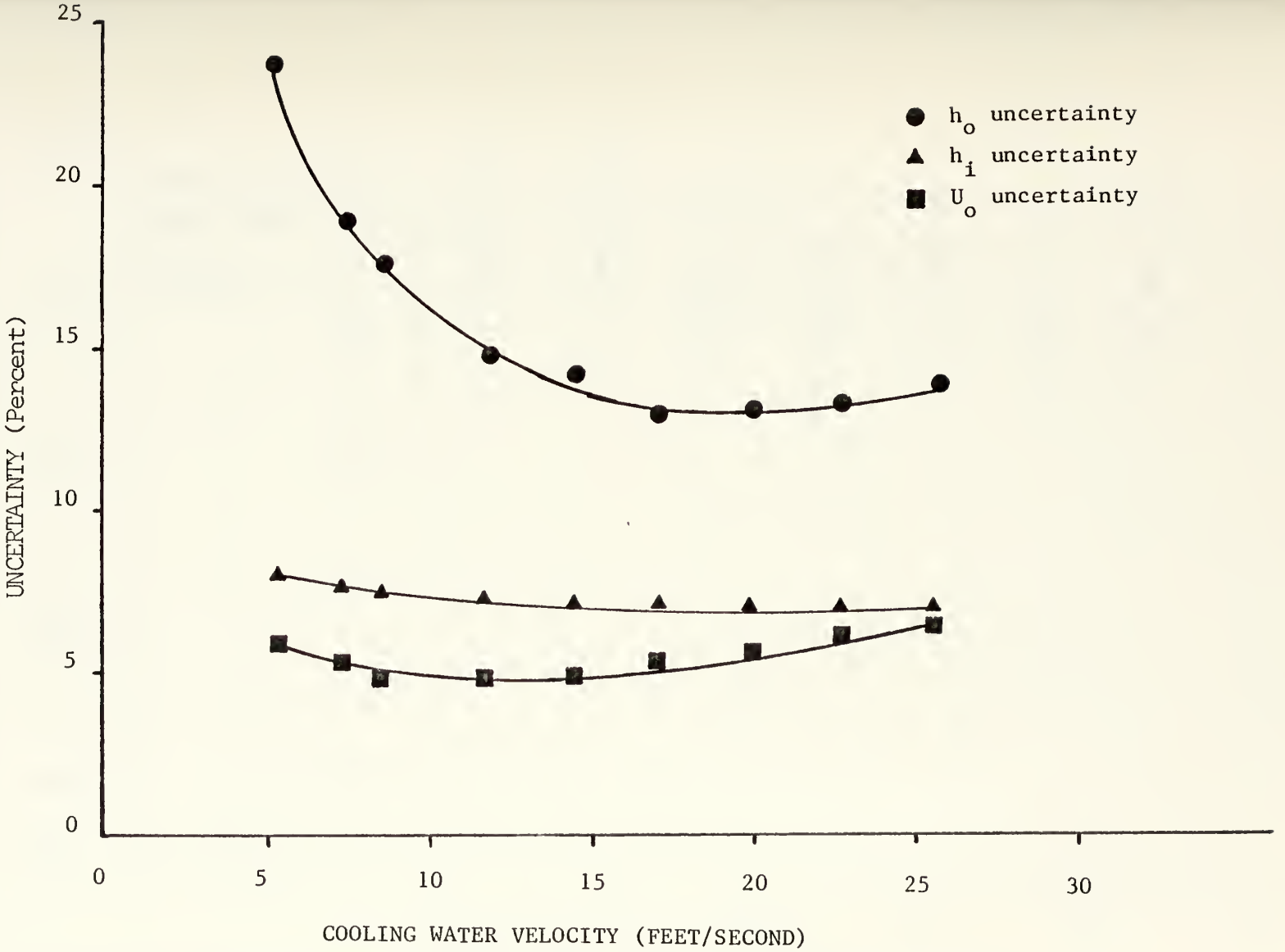


Figure 24. Uncertainties of $U_o$, $h_i$ and $h_o$ Versus Cooling Water Velocity.

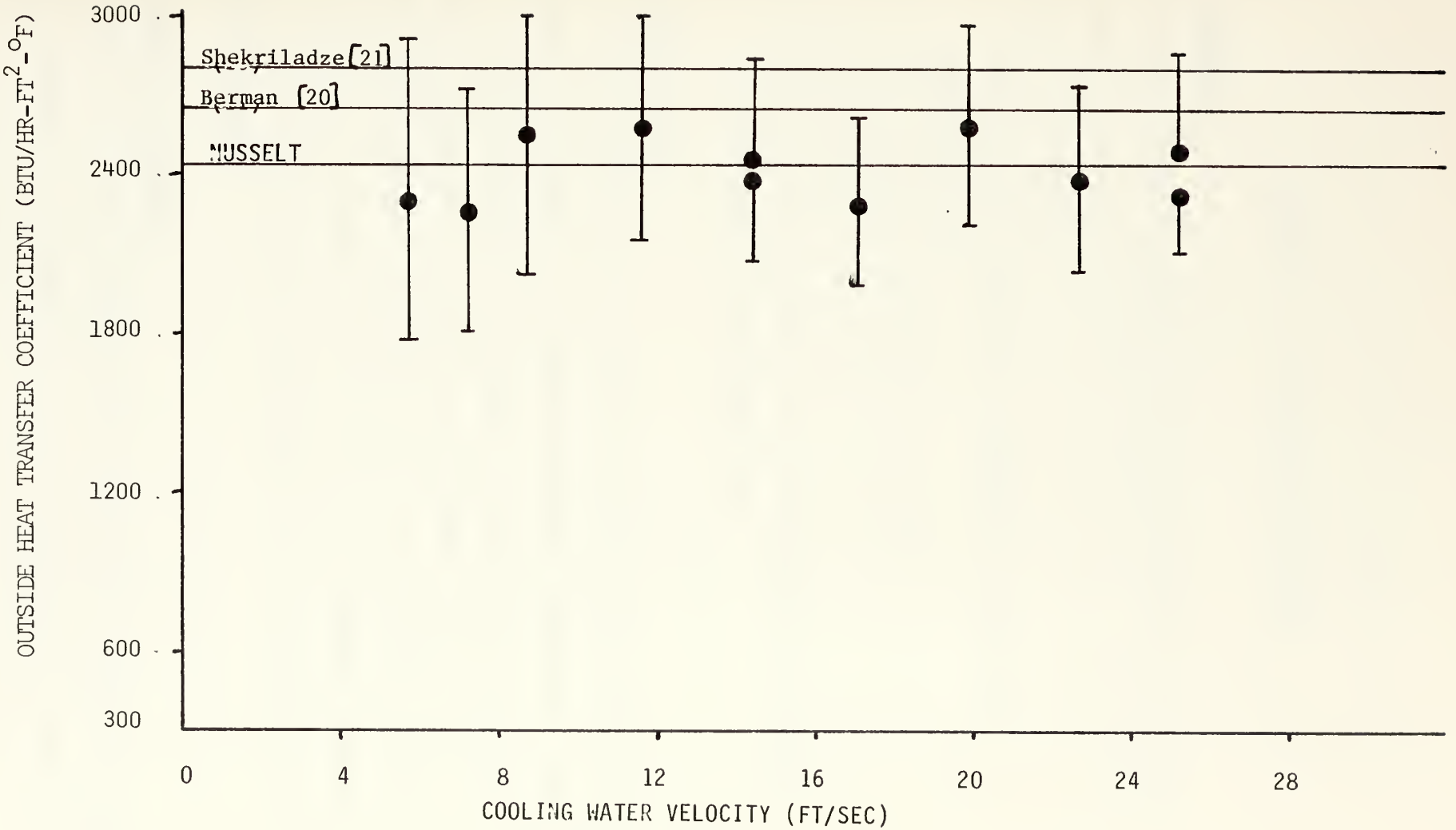


Figure 25. Outside Heat Transfer Coefficient Versus Cooling Water Velocity for Run 5.

## APPENDIX A: CALIBRATION PROCEDURES

### 1. Rotameters

The two rotameters installed in the test condenser and by-pass lines were calibrated by the use of scale and stop watch. The procedure that was used is as follows:

a. Establish flow through the rotameter at a specified percentage level.

b. Record weight of container at time zero.

c. Record weight of container at time t.

d. Flow rate for specified level was determined by dividing the weight gain by the elapsed time.

### 2. Thermocouples

All thermocouples used in this test apparatus were calibrated in a silicone oil bath against a platinum resistance thermometer. The output of the platinum resistance thermometer was determined by the use of a Wheatstone bridge and is accurate to the nearest $0.02^{\circ}F$ ($0.01^{\circ}C$). The Autodata Nine Recorder, the output device for all sheathed thermocouples, is accurate to the nearest $0.2^{\circ}F$ ($0.1^{\circ}C$), and all sheathed thermocouples were found to record the same temperature that was indicated by the platinum standard.

### 3. Pressure Transducer

Calibration of the absolute pressure transducer was done by using a mercury manometer. The amplifier for the transducer had an excitation

voltage of 16.2 volts. A second voltage setting was used to set the scale of the output, and this was set so that the output corresponded to centimeters of mercury. The calibration showed a linear relationship between the transducer and the actual pressure. The output of the transducer when multiplied by ten is equal to the pressure in centimeters of mercury.

## APPENDIX B: OPERATING PROCEDURES

1. Light-off

   a. Using Boiler

      (1) Energize main circuit breaker located in power panel P-2.

      (2) Turn key switch on--located on right side of main control board.

      (3) Energize circuit breaker on left side of main control panel by depressing start.

      (4) Energize individual circuit breakers on left side of main control panel. The following lists the identification of each circuit breaker:

         (a) Feed pump

         (b) Outlets

         (c) Hot water heater (feedwater tank)

         (d) Condensate pump

         (e) Boiler

      (5) Energize circuit breaker for cooling water pump on power panel P-5 (only when using closed cooling water system).

      (6) Insure water level is up in the feedwater tank. Turn switch on to energize heater.

      (7) Energize instrumentation.

         (a) Autodata 9 machine and amplifier.

         (b) Multichannel pyrometer.

      (8) Open valves FW-1 and FW-2, and energize switch to feed pump to recirculate water in feedwater tank.

(9) Insure nitrogen level in cold trap is at full mark (if installed) and start vacuum pump.

(10) After feedwater tank has reached a temperature of 140°F, open valve FW-4, and insure water level in boiler is above low level mark and energize boiler.

(11) Start vacuum pump.

(12) Open valve DS-1.

b. Using House Steam

Follow steps (1) through (5), (7) and (9) as outlined for procedure using boiler.

2. Operation

a. Cooling Water System

(1) Open valve CW-1; then open valve CW-2 one turn to prime the cooling water pump, keeping valves CW-3 and CW-4 closed.

(2) Energize pump, and close valve CW-2. Open valve CW-3 one turn until flow is established, then open valve CW-4 to purge air.

(3) Open valves CW-3 and CW-4 to obtain desired flow rates.

(4) When using the house water supply remove plug from sump and open valve CW-2 with valve CW-1 closed. Follow step 3.

b. Steam System

(1) Using Boiler

(a) When boiler has reached the desired pressure (approximately 3 psig) open valve MS-1.

(b) Insure valves MS-6 and MS-5 are open.

(c) Open valve MS-3 to obtain desired steam flow rate to test condenser. Open valve MS-4 as necessary to maintain boiler pressure at desired level.

(2) Using House Steam

(a) Insure valve MS-1 is closed. Open valve MS-2.

(b) Follow steps (b) and (c) for boiler use.

c. Condensate and Feedwater System

(1) Using Boiler

(a) To collect drains in test condenser hotwell operate with valve C-1 closed. After test run has been completed, open valve and condensate will drain into secondary condenser.

(b) The condensate pump is operated intermittently, when level in secondary condenser dictates. When pump is secured, keep valve C-2 closed. When pump is required, start pump and then open valve C-2 to pressure vacuum. In this mode keep valve C-3 closed.

(c) While feed pump is running (continuous operation) valve FW-1 must be fully open and valve FW-2 must be throttled so that a positive flow is insured. Valve FW-3 is a solenoid valve which is actuated by the boiler controls.

(d) When boiler is energized, valve FW-4 must be fully open.

(e) Make-up is added to the system through the top of the feedwater tank by removing anode.

(2) Using House Steam

(a) Follow step (a) for using boiler.

(b) To pump condensate from secondary condenser hotwell, start pump, and open valve C-3. In this mode keep valve C-2 closed.

(c) Delete steps (c) through (e) for using boiler.

3. Securing System

a. Using Boiler

(1) Close valves MS-3 and MS-4. Close valve MS-1 and secure power to boiler.

(2) Pump condensate from secondary condenser hotwell to feedwater tank. Secure valve C-2.

(3) Secure power to heater.

(4) Secure vacuum pump.

(5) Secure cooling water pump or close valve CW-2 when using house water supply. Close valves CW-3 and CW-4.

(6) Secure instrumentation.

(7) Bottom blow boiler to remove deposits. Repeat twice, blowing from high water mark to low water mark.

(8) Secure power to feed pump.

(9) De-energize individual circuit breakers.

(10) De-energize circuit breaker on control panel; depress stop. Turn key switch off.

b. Using House Steam

(1) Close valve MS-2.

(2) Pump condensate into return line; close valve C-3.

(3) Follow steps (4) through (6), (9) and (10) as outlined for procedure using boiler.

4. Secondary Systems

a. Vacuum System

Vacuum is established by mechanical vacuum pump and is controlled by a vacuum regulator mounted on instrument board mounted by test condenser.

b. Desuperheater

Valve DS-1 controls flow of feedwater (140°F) to spray nozzles. Optimum flow level is between 15 and 20 percent flow on rotameter. Condensate is collected in a small tank below desuperheater so the mass flow rate can be determined.

5. Safety Devices

a. Emergency Power Shut-Off

To secure all power to the system in an emergency, depress the red button on the right side of the main control panel.

b. Boiler

(1) The mercury switches mounted on the main control panel secure power to the heating elements of the boiler when the steam pressure exceeds 25 psig. Power is restored to the heating elements when the pressure drops to approximately 15 psig.

(2) A low water level limit switch is contained within the boiler; and when the water level inside the boiler drops below a preset level, power is secured to the boiler and will not be restored until the water level is above this preset height.

(3) The relief valve mounted on the boiler is set to lift at 30 psig.

6. Instrumentation

a. The Autodata 9 is an automatic recording device with a digital output. This machine records all test temperatures and the test condenser pressure. The following listing gives the output of each of the active channels:

| Channel | Output |
|---|---|
| 1 | Test Condenser Pressure (cm of Hg x $10^{-1}$) |
| 40 | Cooling Water Inlet Temperature ($^{o}$C) |
| 41 | Cooling Water Outlet Temperature ($^{o}$C) |
| 42 | Cooling Water Outlet Temperature ($^{o}$C) |
| 43 | Cooling Water Outlet Temperature ($^{o}$C) |
| 44 | Cooling Water Outlet Temperature ($^{o}$C) |
| 45 | Test Condenser Steam Temperature ($^{o}$C) |
| 46 | Test Condenser Steam Temperature ($^{o}$C) |
| 47 | Test Condenser Steam Temperature ($^{o}$C) |
| 48 | Test Condenser Steam Temperature ($^{o}$C) |
| 49 | Test Condenser Steam Temperature ($^{o}$C) |
| 50 | Test Condenser Steam Temperature ($^{o}$C) |
| 51 | Test Tube Wall Temperature ($^{o}$C) |

b. Main Control Board

(1) The multi-channel pyrometer is powered from the outlets and has a switch located on the front panel. All thermocouples wired to the pyrometer are teflon coated copper-constantan, and they monitor temperatures for system operation. The following is a list of the active channels and their outputs:

| Channel | Output |
|---|---|
| 1 | Secondary Condenser Hotwell ($^{o}$F) |
| 2 | Feedwater Tank ($^{o}$F) |
| 4 | Cooling Water Inlet Temperature ($^{o}$F) |
| 5 | Cooling Water Outlet Temperature ($^{o}$F) |
| 7 | Test Condenser Steam Temperature ($^{o}$F) |
| 6 | Heat Exchanger Water Inlet Temperature ($^{o}$F) |
| 8 | Heat Exchanger Water Outlet Temperature ($^{o}$F) |

(2) The single channel iron-constantan pyrometer displays the boiler steam temperature ($^{o}$F).

(3) The Bourdon tube pressure gauge displays the boiler steam pressure in psig.

(4) Two rotameters are mounted on the main control panel to measure cooling water flow rates.

(a) The rotameter on the left has a capacity of 18.6 gal/min and indicates the flow rate through the test tube.

(b) The rotameter on the right has a capacity of 86 gal/min and indicates the flow rate through the by-pass loop.

c. Auxiliary Instrument Board

The auxiliary instrument board is mounted on the test condenser stand and has the following instrumentation:

(1) Absolute mercury manometer to measure the test condenser pressure.

(2) Mercury manometer to measure the differential pressure drop across the test tube.

(3) Two compound pressure gauges: top one measures pressure in calorimeter and, bottom one measures the pressure in the secondary condenser.

(4) Vacuum control regulator to control the pressure inside the test condenser by injecting air into the suction of the vacuum pump.

d. Annubar - Steam Flow Measuring Device

An inclined water manometer is connected to the Annubar to measure the differential pressure across the Annubar. The following equation is used to determine the steam mass flow rate through the Annubar [22]:

$$W_N = 0.1266\ SND^2F_AF_MV_a\sqrt{\gamma_f}\ \sqrt{h_n}$$

where

$S = 0.638$

$N = 2835$

$D = 1.25"$

$F_A$ = see reference 22

$F_M$ = see reference 22

$V_a = 1.00$

$\sqrt{\gamma_f}$ = see reference 22

$h_n$ = differential pressure ("$H_2O$)

## APPENDIX C: UNCERTAINTY ANALYSIS

The general form of the Kline and McClintock [23] "second order" equation is used to compute the uncertainty. If the resultant, R, is some function of primary variables $x_1, x_2, \ldots, x_n$, then the uncertainty in R, $\delta R$, is given by:

$$\delta R = \left[\left(\frac{\partial R}{\partial x_1}\delta x_1\right)^2 + \left(\frac{\partial R}{\partial x_2}\delta x_2\right)^2 + \ldots + \left(\frac{\partial R}{\partial x_n}\delta x_n\right)^2\right]^{\frac{1}{2}} \qquad \text{(C-1)}$$

where $\delta x_1, \delta x_2, \ldots, \delta x_n$ are the uncertainties in each of the measured variables $x_1, x_2, \ldots, x_n$.

The overall heat transfer coefficient is given by equation (7).

$$U_o = \frac{m_c c_p}{A_o} \ln \frac{T_s - T_{ci}}{T_s - T_{co}}$$

By applying equation (C-1) to equation (7), the following equation results:

$$\frac{\delta U_o}{U_o} = \left[\left(\frac{\delta A_s}{A_s}\right)^2 + \left(\frac{\delta c_p}{c_p}\right)^2 + \left(\frac{\delta m_c}{m_c}\right)^2 + \left\{\frac{\delta T_s (T_{ci} - T_{co})}{(T_s - T_{ci})(T_s - T_{co}) \ln \frac{T_s - T_{ci}}{T_s - T_{co}}}\right\}^2 + \right.$$

$$\left.\left\{\frac{\delta T_{co}}{(T_s - T_{co}) \ln \frac{T_s - T_{ci}}{T_s - T_{co}}}\right\}^2 + \left\{\frac{\delta T_{ci}}{(T_s - T_{ci}) \ln \frac{T_s - T_{ci}}{T_s - T_{co}}}\right\}^2\right]^{\frac{1}{2}} \qquad \text{(C-2)}$$

The following were the uncertainties assigned to the variables:

$$\delta c_p = 0.001 \text{ BTU/lbm-}^{\circ}\text{F}$$

$$\delta m_c = 0.01 \ \dot{m}_c \text{ lbm/hr}$$

$$\delta T_s = 0.2 \ ^{\circ}\text{F}$$

$$\delta T_{co} = 0.2 \ ^{\circ}\text{F}$$

$$\delta T_{ci} = 0.2 \ ^{\circ}\text{F}$$

$$\delta A_o = 0.008 \text{ ft}^2$$

By applying equation (C-1), the uncertainty for the Reynolds number is given by:

$$\frac{\delta Re}{Re} = \left[\left(\frac{\delta m_c}{m_c}\right)^2 + \left(\frac{\delta \mu}{\mu}\right)^2 + \left(\frac{\delta D_i}{D_i}\right)^2\right]^{\frac{1}{2}} \qquad \text{(C-3)}$$

where

$$\delta m_c = 0.01 \ m_c \text{ lbm/hr}$$

$$\delta \mu = 0.01 \text{ lbm/ft-hr}$$

$$\delta D_i = 0.005 \text{ inches}$$

The uncertainty for the coefficient, $C_i$, is given by:

$$\frac{\delta C_i}{C_i} = \left[\left(\frac{\delta D_o}{D_o}\right)^2 + \left(\frac{\delta_{slope}}{slope}\right)^2 + \left(\frac{\delta k}{k}\right)^2\right]^{\frac{1}{2}} \qquad \text{(C-4)}$$

where

$$\delta D_o = 0.005 \text{ inches}$$

$$\delta k = 0.001 \text{ BTU/hr-ft-}^{\circ}\text{F}$$

$$\delta_{slope} = 0.065 \text{ slope}$$

Applying equation (C-1) to equation (8) results in the following expression:

$$\frac{\delta h_i}{h_i} = \left[ \left(\frac{\delta k}{k}\right)^2 + \left(\frac{\delta D_i}{D_i}\right)^2 + \left(\frac{\delta C_i}{C_i}\right)^2 + \left(\frac{0.8\delta Re}{Re}\right)^2 + \left(\frac{0.33\delta Pr}{Pr}\right)^2 + \left\{\frac{\delta(\mu/\mu_w)}{(\mu/\mu_w)}\right\}^2 \right]^{\frac{1}{2}} \qquad \text{(C-5)}$$

where

$\delta k$ = 0.001 BTU/hr-ft-$^{o}$F

$\delta D_i$ = 0.005 inches

$\delta C_i \equiv$ from equation (C-4)

$\delta Re \equiv$ from equation (C-3)

$\delta Pr$ = 0.01

$\delta(\mu/\mu_w)$ = 0.01

Applying equation (C-1) to equation (11) results in the following expression:

$$\frac{\delta h_o}{h_o} = \left[ \left\{ \frac{\delta U_o}{U_o^2 \left(\frac{1}{U_o} - R_w - \frac{D_o}{D_i h_i}\right)} \right\}^2 + \left\{ \frac{\delta R_w}{\left(\frac{1}{U_o} - R_w - \frac{D_o}{D_i h_i}\right)} \right\}^2 + \left\{ \frac{\left(\frac{D_o}{D_i h_i}\right)\left(\frac{\delta h_i}{h_i}\right)}{\left(\frac{1}{U_o} - R_w - \frac{D_o}{D_i h_i}\right)} \right\}^2 \right]^{\frac{1}{2}} \qquad \text{(C-6)}$$

where

$\delta U_o \equiv$ from equation (C-2)

$\delta R_w \equiv 9 \times 10^{-6}$ he-ft$^2$-$^{o}$F/BTU

$\delta h_i \equiv$ from equation (C-5)

## APPENDIX D: SAMPLE CALCULATIONS

The following are the calculations for the isothermal pressure drop for runs 1, 2 and 5 for a flow rate of 50 percent

$$f = \Delta p \, g_c / 2\rho V^2 (L/D_i)$$

$T_{co} = 68.9^{\circ}F$

$L = 51.125"$

$D_i = 0.521"$

$\rho = 62.3 \text{ lb/ft}^3$

| $\Delta p$ ("Hg) | correction ("Hg) | $\Delta p$ psf | V (ft/sec) | f |
|---|---|---|---|---|
| 6.30 | 0.5 | 410.22 | 14.27 | 0.0053 |

The following heat transfer calculations are for run 5 with a 50 percent flow rate.

Determination of the overall heat transfer coefficient:

$$U_o = \frac{m_c c_p}{A_o} \ln \frac{T_s - T_{ci}}{T_s - T_{co}}$$

where $T_s = 144.5^{\circ}F$

$T_{ci} = 76.8^{\circ}F$

$T_{co} = 83.7^{\circ}F$

$$T_f = \frac{T_{ci} + T_{co}}{2} = 80.3^{\circ}F$$

$$\ln \frac{T_s - T_{ci}}{T_s - T_{co}} = 0.1075$$

$$\dot{m}_c = 1.316 \text{ lbm/sec}$$

$$A_o = \pi D_o L = 0.4908 \text{ ft}^2$$

$$c_p = 0.999 \text{ BTU/lbm-}^\circ\text{F}$$

$$U_o = \frac{(1.316 \text{ lb/sec})(3600)(0.999 \text{ BTU/lbm-}^\circ\text{F})}{0.4908 \text{ ft}^2} (0.1075)$$

$$= 1037 \text{ BTU/hr-ft}^2\text{-}^\circ\text{F}$$

Determination of Wilson Plot Abscissa ($Re^{-0.8} Pr^{-1/3} (\mu/\mu_w)^{-0.14}$)

$$Re = \frac{\rho V D_i}{\mu} = \frac{\rho D_i (m_c/\rho A)}{\mu} = \frac{4m_c}{\pi \mu D_i} = 67{,}118$$

where

$$D_i = 0.521"$$

$$\mu = 2.07 \text{ lbm/ft-hr}$$

$$Pr = 5.82$$

$$\mu_w = 1.24 \text{ lbm/ft-hr}$$

$$Re^{-0.8} Pr^{-1/3} (\mu/\mu_w)^{-0.14} = 0.713 \times 10^{-4}$$

Determination of inside heat transfer coefficient, $h_i$:

$$h_i = \frac{k}{D_i} C_i Re^{0.8} Pr^{1/3} (\mu/\mu_w)^{0.14}$$

where

$$k = 0.355 \text{ BTU/hr-ft-}^\circ\text{F}$$

$$D_i = 0.521"$$

$$C_i = 0.028$$

$$h_i = \frac{0.355}{(0.521/12)} (0.028)(14.025 \times 10^3)$$

$$= 3211 \text{ BTU/hr-ft}^2\text{-}^\circ\text{F}$$

Determination of outside heat transfer coefficient, $h_o$:

$$h_o = \frac{1}{\frac{1}{U_o} - R_w - \frac{D_o}{D_i h_i}}$$

where

$$R_w = \frac{D_o \ln r_o/r_i}{2k_w} = \frac{0.625 \ln 0.625/0.521}{(12)(2)(25.8)} = 1.837 \times 10^{-4}$$

$$h_o = \frac{1}{9.64\text{x}10^{-4} - 1.837\text{x}10^{-4} - \frac{0.625}{0.521(3211)}} = 2453 \text{ BTU/hr-ft}^2\text{-}^\circ\text{F}$$

# BIBLIOGRAPHY


1. Search, H. T., A Feasibility Study of Heat Transfer Improvement in Marine Steam Condensers, MSME, Naval Postgraduate School, December 1977.

2. Bergles, A. E. and Jensen, M. K., Enhanced Single-Phase Heat Transfer for Ocean Thermal Energy Conversion Systems, Report HTL-13, ISU-ERI-Ames-77314, ERI Project 1278, April 1977.

3. Bergles, A. E., Survey of Augmentation of Two-Phase Heat Transfer, paper presented at ASHRAE Semi-Annual Meeting, Dallas, Texas, February 1976.

4. Palen, J., Cham, B., and Taborek, J., Comparison of Condensation of Steam on Plain and Turbotec Spirally Grooved Tubes in a Baffled Shell-and-Tube Condenser, Heat Transfer Research, Inc. Report 2439-300/6, January 1971.

5. Eissenberg, D. M., An Investigation of the Variables Affecting Steam Condensation on the Outside of a Horizontal Tube Bundle, Ph.D. dissertation, University of Tennessee, December 1972.

6. Newson, I. H. and Hodgson, T. K., The Development of Enhanced Heat Transfer Condenser Tubing, 4th International Symposium on Fresh Water from the Sea, Vol. 1, 69-94, 1973.

7. Watkinson, A. P., Miletti, D. L. and Tarasoof, P., Heat Transfer and Pressure Drop of Internally Finned Tubes, AIChE Symposium Series, No. 131, Vol. 69, 1973.

8. Catchpole, J. P. and Drew, B.C.H., Evaluation of Some Shaped Tubes for Steam Condensers, paper from British Ministry of Defense, 1974.

9. Young, E. H., Withers, J. G. and Lampert, W. B., Heat Transfer Characteristics of Corrugated Tubes in Steam Condensing Applications, AIChE Paper No. 3, August 11, 1975.

10. Rothfus, R. R., Concurrent Studies of Enhanced Heat Transfer and Materials for Ocean Thermal Exchangers, ERDA Contract No. EY-76-S-02-2641-1, 31 July, 1976.

11. YIM Heat Exchanger Tubes: Design Data for Horizontal Roped Tubes in Steam Condensers, Technical Memorandum 3, Yorkshire Imperial Metals Limited, December 1975.

12. Beck, A. C., A Test Facility to Measure Heat Transfer Performance of Advanced Condenser Tubes, MSME thesis, Naval Postgraduate School, December 1976.

13. Smithells, C. J., Metals Reference Book, 3rd Ed., Vol. 2, p. 1030, Buttersworth, 1962.

14. Knudsen, J. G. and Katz, D. L., Fluid Dynamics and Heat Transfer, pp. 332-335, McGraw-Hill Book Company, 1958.

15. Standard Handbook for Mechanical Engineers, 7th ed., T. Baumeister, Ed.-in-chief, McGraw-Hill, 1967.

16. Jackson, R. M., Condensing Heat Transfer Rates of Tubes of Various Materials, Evaluation Report 030038, NS-643-078, United States Naval Engineering Experiment Station, 12 July 1956.

17. Holman, J. P., Heat Transfer, 3rd ed., McGraw-Hill, 1972.

18. Withers, J. G. and Young, E. H., Investigation of Steam Condensing on Vertical Rows of Horizontal Corrugated and Plain Tubes, Symposium on Enhanced Tubes for Desalination Plants, July 1970.

19. Eissenberg, D. M., The Multitube Condenser Test, Symposium on Enhanced Tubes for Desalination Plants, July 1970.

20. Berman, L. D. and Tumanov, Y. K., Investigation of the Heat Transfer with Condensation of Flowing Steam on a Horizontal Tube, Teploenergetika, 9:77, 1962.

21. Shekriladze, I. G. and Zhorzholiani, G. I., Analysis of the Process of Film Condensation of Moving Vapor on a Horizontal Cylinder, Inzhenerno-Fizicheskii Zhurnal, Vol. 25, No. 1, pp. 14-19, July 1973.

22. Ellison Instrument Division Dietrich Standard Corp., Calculation Report E-78, Section D. Annubar Flow Calculation Report, 1968.

23. Kline, S. J. and McClintock, F. A., Describing Uncertainties in Single Sample Experiments, Mech. Engin., Vol. 74, p. 3-8, January 1953.

INITIAL DISTRIBUTION LIST

| | | No. Copies |
|---|---|---|
| 1. | Defense Documentation Center<br>Cameron Station<br>Alexandria, Virginia 22314 | 2 |
| 2. | Library, Code 0142<br>Naval Postgraduate School<br>Monterey, California 93940 | 2 |
| 3. | Department Chairman, Code 69<br>Department of Mechanical Engineering<br>Naval Postgraduate School<br>Monterey, California 93940 | 2 |
| 4. | Office of Research Administration, Code 012A<br>Naval Postgraduate School<br>Monterey, California 93940 | 1 |
| 5. | Professor Paul J. Marto, Code 69Mx<br>Department of Mechanical Engineering<br>Naval Postgraduate School<br>Monterey, California 93940 | 10 |
| 6. | LT. Derry T. Pence, USN<br>1247 Spruance Road<br>Monterey, California 93940 | 4 |
| 7. | CDR N. P. Nielsen, USN<br>Naval Sea Systems Command (033)<br>2221 Jefferson Davis Hwy, CP#6<br>Arlington, Virginia 20360 | 1 |
| 8. | Mr. Charles Miller<br>Naval Sea Systems Command (0331)<br>2221 Jefferson Davis Hwy, CP#6<br>Arlington, Virginia 20360 | 2 |
| 9. | Mr. Frank Ventriglio<br>Naval Sea Systems Command (0331)<br>2221 Jefferson Davis Hwy, CP#6<br>Arlington, Virginia 20360 | 1 |
| 10. | Mr. Arthur Chaikin<br>Naval Sea Systems Command (0331)<br>2221 Jefferson Davis Hwy, CP#6<br>Arlington, Virginia 20360 | 1 |

11. CAPT J. K. Parker, USN — 1
Naval Sea Systems Command (PMS-301)
2221 Jefferson Davis Hwy, CP#6
Arlington, Virginia 20360

12. CDR D. W. Barns, USN — 1
Naval Sea Systems Command (PMS-301.3)
2221 Jefferson Davis Hwy, CP#6
Arlington, Virginia 20360

13. Mr. Walter Aerni — 1
Naval Ship Engineering Center (6145)
Washington, D. C. 20362

14. Mr. Wayne L. Adamson — 1
Naval Ship Research & Development Center (2761)
Annapolis, Maryland 21402

15. Mr.Gil Carlton — 1
Naval Ship Engineering Center (6723)
Philadelphia, Pennsylvania 19112

16. Dr. David Eissenberg — 1
Oak Ridge National Laboratory
Post Office Box Y
Oak Ridge, Tennessee 37830

17. Mr. Joseph A. Hafford — 1
Oak Ridge National Laboratory
Post Office Box Y
Oak Ridge, Tennessee 37830

18. Mr. John W. Ward — 1
Marine Division
Westinghouse Electric Corporation
Hendy Avenue
Sunnyvale, California 94088

19. Mr. Henry Braun — 1
De Laval Condenser and Filter Division
Florence, New Jersey 08518

20. Miss Eleanor J. Macnair — 1
Ship Department
Ministry of Defence
Director - General Ships - Block B
Foxhill, Bath, Somerset
ENGLAND

21. Mr. Kurt Bredehorst — 1
NAVSEC 6147D
Department of the Navy
Hyattsville, Maryland 02782

Thesis
P3293
c.1
Pence
174935
An experimental study of steam condensation on a single horizontal tube.